A STUDY OF SPACE COMMUNICATIONS SPREAD-SPECTRUM SYSTEMS

(Phases 5 and 6)

Part 2 Coding and Modulation

FINAL PROGRESS REPORT

Department of Electrical Engineering

Queen's University at Kingston

Kingston, Ontario, Canada

A STUDY OF SPACE COMMUNICATIONS SPREAD-SPECTRUM SYSTEMS

(Phases 5 and 6)

Part 2 Coding and Modulation

FINAL PROGRESS REPORT

P.H. Wittke
M. Schefter
Y.M. Lam

Report No. 90-2

March 1990

Prepared for

The Department of Communications

Under DSS Contract No. 36001-8-3528/01-SS

Department of Electrical Engineering

Queen's University

Kingston, Ontario, Canada

TABLE OF CONTENTS

A STUDY OF SPACE COMMUNICATIONS SPREAD-SPECTRUM SYSTEMS

Part 2 - Coding and Modulation

SUMMARY

Trellis codes are obtained for use with noncoherent m-ary FSK transmission. These codes give improved performance in additive noise but they do not require an increased bandwidth. The current task under Part B. of the work statement - Coding and Modulation, is

1. to investigate trellis-like codes to improve immunity to jamming.

For Phase 6, additional areas of investigation were identified:

2. to analyze and simulate the effects of the number of code states on performance of NCFSK trellis coded modulation.
3. to investigate the utilization of estimated jammer information in decoding.

This part, Part 2 of the Interim Report, reports the progress achieved in this area since the work was started in October 1988.

Our goal in the current work is to find the performance of trellis-coded noncoherent frequency-shift keying (NCFSK) as would be used in a hopped spread spectrum system, in the presence of jamming and with a range of possible detection metrics or schemes that will be effective in a jamming environment. In particular, in our trellis coding, we expand the signal set for noncoherently orthogonal M-ary FSK to 2M-ary noncoherent FSK. The tones are uniformly spaced, but to avoid significant bandwidth expansion, nonorthogonal tone spacing is permitted. For example, the tone spacing is reduced from the usual spacing of 1/T Hz to 1/2T, 1/3T or 2/3T Hz. The performance of 4-ary NCFSK with 2-state, 4-state and 8-state trellis coding is evaluated and the effects of tone spacing on error performance is investigated. The decoding metric employed is the simple energy metric. Performance in the presence of noise is analyzed and it is concluded that a coding gain of from 2 - 4 dB. can be achieved with a simple 4-state trellis code. The exact gain depends on the choice of signal spacing.

In a jamming environment, the coding gains are much more dramatic. For partial band noise jamming, a noncoherent receiver which is able to detect the presence of jamming in the band, is considered. The performance analysis is based on the union Chernoff bound on the probability of bit error. The bound has been extended to take into account the fact that the signals are not orthogonal. A transfer function bound is derived for the present case of trellis coding and noncoherent detection. Very substantial performance improvements are indicated by use of trellis coding in worst case partial band noise jamming. Simulations have been carried out which yield performance within a fraction of a dB. of that predicted by the bounds. A practical self-normalizing decoding metric is shown to give performance very close to that predicted by the idealized jamming bound considerations. There is significant improvement in a 4-state over a 2-state code, but little improvement is seen in going from 4-state to 8-state codes.

A STUDY OF SPACE COMMUNICATIONS SPREAD-SPECTRUM SYSTEMS

Part 2 - Coding and Modulation

Statement of Work:

A previous contract identified possible issues to be investigated in three areas:

A. Uplink Synchronization

B. Coding and Modulation

C. Surface-acoustic Wave Block Demodulation.

In particular, previous coding and modulation work obtained trellis codes for use with noncoherent m-ary FSK, that give improved performance in additive noise and do not require an increased bandwidth. The task under Part B. Coding and Modulation starting with Phase 5 of the Contract, was:

1. to investigate trellis-like codes to improve immunity to the three types of jamming: partial-band noise, tone and pulse jamming.

For Phase 6, additional areas of investigation were identified:

2. to analyze and simulate the effects of the number of code states on performance of NCFSK trellis coded modulation.
3. to investigate the utilization of estimated jammer information in decoding.

This Final Report summarizes the progress achieved in Coding and Modulation since the contract started in October 1988. The general analysis technique was reported in an earlier Interim Progress Report [1]. It is included here for completeness and since the final report includes simulation results that should be compared with theory. In addition, in this final phase, error bounds that are significantly tighter than those reported in [1] are derived and evaluated.

I. INTRODUCTION

The use of spread spectrum communications to combat jamming is well-known and much of the on-going research in military satellite communications

(MILSATCOM) has been focused on frequency-hopped systems [2-17]. Hopping the carrier frequency over a wide band results in an improved error performance against a simple jammer which must distribute its power thinly over a wide band in order to jam the signal. However, it is well-known [2, vol.II, pp.73-94; 2, pp.574-582 and pp.597-602] that the performance of uncoded frequency-hopped systems can suffer degradations of the order of 30 - 50 dB at typical operating points when confronted with more sophisticated jammers such as, for example, a partial band noise jammer which jams a fraction of the bandwidth and brings greater degradation to the communications system. Worst-case partial band noise jamming involves balancing the probability of jamming a given hop against the effective strength of jamming power for a fixed total jammer power.

Under worst case partial band noise jamming, the choice of modulation alone makes little difference in error performance [4, 5, 6 p.173]. The use of coding is extremely important when considering the worst case performance against an intelligent jammer. Evaluation of the coded error probabilities for antijam communications systems shows that gains of the order of 30-40 dB can be obtained over uncoded systems [7-10]. Besides error correcting coding [7-15], diversity [5,9,14,15] and interleaving [14] have also been utilized to enhance the protection against partial band or pulsed jammers. When coding is employed, various decoding metrics [9,16] for use in a jamming environment have been devised. The most popular decoding metrics under study are: the hard decision metric with and without side information [8,11], and Viterbi ratio threshold techniques with erasure and quality bits [12]. More recently, a robust metric called the square-law self-normalized energy metric [9,10,17] has also received attention. Results on its performance will be given in this report.

The ability to detect or correct errors can be provided only by the transmission of additional redundant bits and thus by lowering the effective information rate per transmission bandwidth. Conventional hard decision encoders and decoders for error correction operate on binary, or more generally m-ary, code symbols transmitted over a discrete channel. However, when modulation and error-correcting coding are performed in the classical independent manner, disappointing results are obtained. The reason has been pointed out to be irreversible loss of information in the receiver due to

independent hard symbol decisions made prior to decoding [18]. When coherent detection is utilized another problem is that mapping of code symbols of a code optimized for Hamming distance into nonbinary modulation signals does not guarantee that a good Euclidean distance structure is obtained [18].

Massey [19] was the first to show that considerable performance improvement could be obtained by treating coding and modulation as a single entity. Trellis-coded modulations, so named by Ungerboeck [18,20,21], then evolved as a combined coding and modulation technique for digital transmission over band-limited channels. It can be shown that, in order to get a significant coding gain, it is sufficient that k bits be coded into 2^{k+1} channel signals. The number of channel signals for uncoded modulation is then doubled. Redundancy is provided by the signal-set expansion and in the case of coherent transmission, more bandwidth is not required than for the equivalent uncoded scheme. Coding gains can be obtained with moderate additional complexity.

Early work on trellis-coded modulation [18-23] was primarily on multilevel and multiphase modulations, in order to achieve coding gain without the accompanied sacrifice in band efficiency. Coherent detection was the primary detection scheme considered throughout the development of Ungerboeck's trellis-coded modulation. In the context of frequency hopped systems in MILSATCOM, noncoherent detection is required due to the difficulty of maintaining a coherent carrier phase through the frequency hopping and dehopping processes. In an earlier report [24], work on frequency-hopped FSK with trellis coding and the transmission of combinations of orthogonal FSK tones to avoid any bandwidth expansion, was reported. Significant coding gains were obtained for transmission in additive noise. Results reported were obtained by simulation with only a few analytical results, as the signals were correlated multiple tones for which there are not explicit detection expressions. Our goal in the current work is to find the performance of trellis-coded noncoherent frequency-shift keying (NCFSK) as would be used in a hopped spread spectrum system, in the presence of jamming and with a range of possible detection metrics or schemes, as mentioned above. We wish to avoid exhaustive simulation in the search for good codes and in the examination of a range of techniques for

decoding in a jamming environment. Thus we have chosen to examine trellis coding for the single-tone NCFSK modulation format, which is easier to analyse. As well, this is the modulation commonly proposed for hopped spread spectrum systems.

In this report we consider expanding noncoherently orthogonal M-ary FSK to 2M-ary noncoherent FSK. Nonorthogonal tone spacing is considered to avoid significant bandwidth expansion, and the tones are uniformly spaced. For example, in one case the tone spacing is reduced from the usual spacing of 1/T to 1/2T Hz, and 2 subsets of orthogonal FSK signals are obtained. The bandwidth expansion is small, tending to zero as M increases. For simplicity in analysis, the performance of 4-FSK with 2-state, 4-state and 8-state trellis coding will be evaluated. The effects of tone spacing on error performance is investigated. The soft decision decoding metric employed is the simple energy metric. For partial band noise jamming analysis, a decoder with perfect side information is considered. The performance analysis is based on the union Chernoff bound on the probability of bit error. A transfer function bound [25-27] is derived and used to obtain the union bound. Performance improvement by the use of trellis coding under the usual additive white Gaussian noise will be presented first. Performance under worst case partial band noise jamming will then be presented. In the consideration of convolutional codes in jamming, analysis assuming "perfect side information" is well-known. Although these analyses show the potential of schemes that take into account the jamming, there is concern that practical implementations will fall short of this promise. To respond to these concerns, we include results on a self-normalizing decoding metric derived simply from the usual receiver observations that are passed to the decoder.

Work in the first phase or year of the contract consisted of theoretical work which indicated that substantially enhanced performance could be obtained with trellis coding of an expanded noncoherent signal set where the signal spacing had been reduced so that the frequency allocation required is not significantly increased. The theoretical work as in most coding work, was based on the derivation of performance bounds. In the second year or most recent phase of the contract, work has been focused on evaluation of performance in the presence of jamming and a system simulation

was implemented. New tighter bounds on the performance have been derived. The results of the simulation have corroborated the conclusions based upon bounds and allowed us to conclude that the order of performance promised by our "perfect side information" analyses , can be achieved with simple practical receiver configurations. As well, we are able to simulate jamming situations and receivers that are not amenable to analysis. We have investigated specific system parameters such as the number of states in the codes, as specified in the contract. Our work has stressed performance in full-band and partial-band jamming and work on tone and pulse jamming remains to be carried out.

II. SYSTEM DESCRIPTION

The frequency-hopped system under consideration employs noncoherent frequency-shift-keying (NCFSK) with trellis coding. A system block diagram is shown in Fig. 1. The binary bit stream goes into a rate k/k+1 trellis encoder. The trellis-coded symbols are mapped in groups of (k+1) bits, into an $m=2^{k+1}$ level NCFSK signal set according to the set partitioning method [20]. The carrier frequency of the NCFSK signal is hopped pseudorandomly by the frequency hopper and transmitted. In the receiver, the received signal is dehopped by the frequency dehopper to its original signaling frequency. We consider the hopping rate to be the same as the symbol transmission rate, in this report. Time diversity is not considered here. For NCFSK, the optimum detector is a bank of envelope detectors (or energy detectors which give the square of the envelope) matched to each of the NCFSK signaling frequencies. The energy detector outputs together with any side information about the jamming derived by the receiver go to the trellis decoder, which is simply a maximum metric decoder (e.g. Viterbi decoder). The transmitted data is decoded according to the decision rule employed.

It should be noted that based upon a new description of trellis codes by Calderbank and Mazo [22], the two step processes of specifying an underlying trellis code and mapping the output code symbols into the signal constellation based on the set partitioning rule, can be combined into a single step [23]. The trellis-coded NCFSK signal can be easily produced by a voltage-controlled oscillator (VCO) with the control voltage being a trellis-coded m-ary level signal. The FSK tone spacing is set by the

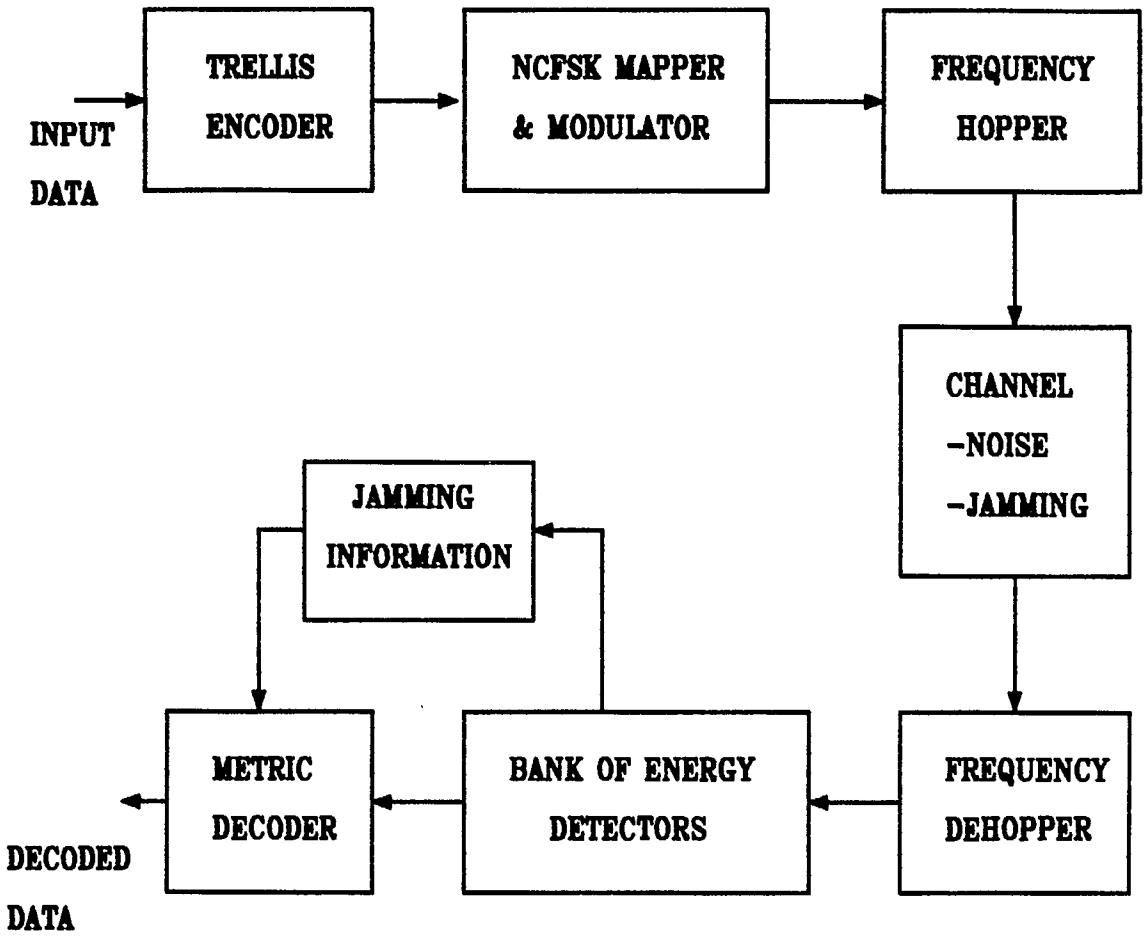

Figure 1: Frequency - hopped trellis - coded noncoherent FSK system block diagram.

amplitude of the trellis-coded modulating signal and the frequency sensitivity of the VCO.

Consider an m-ary NCFSK signal set with uniform tone spacing of Δ Hz. For convenience let S_1 to S_m denote the m NCFSK signals as shown in Fig. 2. During any signaling interval, one of the NCFSK signals in the signal set is transmitted. The signals are given by

$$S_i = \sqrt{2P} \cos [2\pi f_i t + \theta_i] \quad 1 \leq i \leq m , \; 0 < t < T \tag{1}$$

where P is the signal power, f_i is the i^{th} signalling frequency and θ_i is the noncoherent carrier phase of the i^{th} signal. With the signals ordered in the way shown in Fig. 2, the frequency separation between two signals S_i and S_j denoted by Δ_{ij} is given by

$$\Delta_{ij} = |i-j| \, \Delta \tag{2}$$

The cross-correlation coefficient ρ_{ij} of S_i and S_j is given by [28, p.148].

$$\rho_{ij} = \frac{\sin \pi T \Delta_{ij}}{\pi T \Delta_{ij}} \; e^{-j\pi T \Delta_{ij}} \tag{3}$$

Its magnitude is

$$|\rho_{ij}| = \left| \frac{\sin \pi T \Delta_{ij}}{\pi T \Delta_{ij}} \right| = \frac{\sin \pi T \Delta \, |i-j|}{\pi T \Delta \, |i-j|} \tag{4}$$

When the tone spacing $\Delta = \frac{1}{T}$, $|\rho_{ij}| = 0$ for all $i \neq j$, and all NCFSK tones are mutually orthogonal. This gives an expanded signal set with the best error performance. However, the bandwidth occupancy of this orthogonal NCFSK signal set is approximately twice that of the uncoded case. To avoid bandwidth expansion, we consider expanding the uncoded (m/2)-ary NCFSK signals to m-ary NCFSK signals with nonorthogonal tone spacing. According to the set partitioning rule [20], the m-ary signal set is successively partitioned into subsets of signals. The frequency separation between signals is doubled after each level of partitioning as shown in Fig. 2 for m=8.

At the ℓ^{th} level of set partitioning, the frequency spacing of signals in each subset is $2^{\ell} \Delta$ Hz. In particular, if $\Delta = 1/2^{\ell}T$ all signals in each

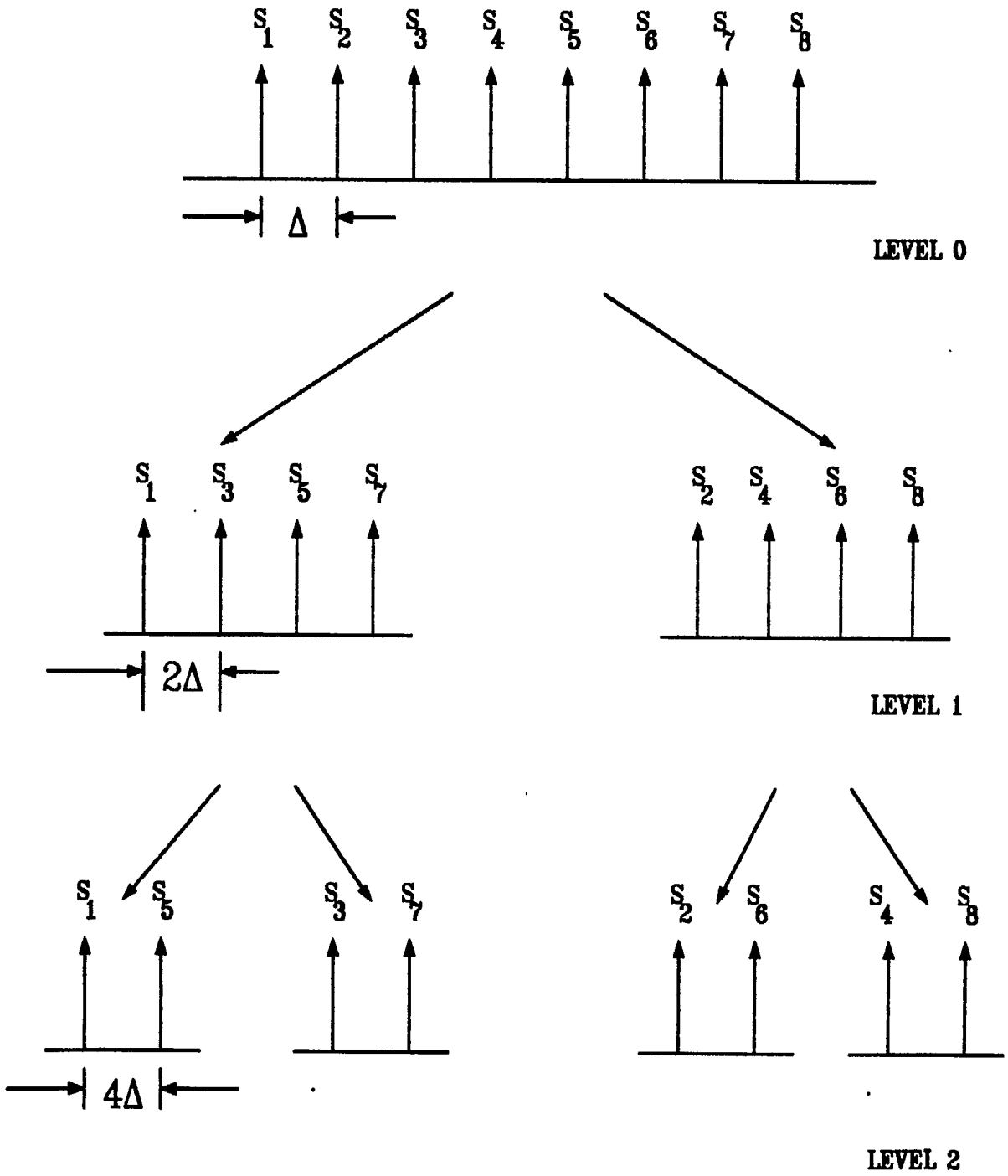

Figure 2: Set partitioning of 8-NCFSK.

subset are orthogonal and there is no advantage in partitioning the signals any further.

For m-ary NCFSK in additive white Gaussian noise, the optimum noncoherent detector is a bank of m envelope or energy detectors. The square of the j^{th} envelope detector output is the energy of the received signal at the j^{th} signalling frequency. Let $U_1, \ldots U_m$ be the outputs of the envelope detectors. Given S_i was transmitted, the output of the j^{th} envelope detector is [28, p. 206]

$$U_j = | \rho_{ij} \sqrt{E} + n_j |, \quad j \neq i, \quad i,j \in [1,m]$$

$$U_i = |\sqrt{E} + n_i | \tag{5}$$

where ρ_{ij} is the complex cross-correlation coefficient of S_i and S_j, E is the signal energy and n_j are complex-valued Gaussian random variables with zero mean and variance $N_o/2$.

The probability density function of the output for the j^{th} envelope detector given S_i was sent, is a Rician-distributed random variable. If U_i is normalized by $(2/N_o)^{1/2}$, the density is given by [28, p.206].

$$p(U_j|S_i) = U_j \exp\{-[U_j^2/2 + |\rho_{ij}|^2 E/N_o]\} I_o(U_j [2E \left|\rho_{ij}\right|^2/N_o]^{1/2}); \quad u_j>0$$
$$= 0; \quad u_j < 0 \tag{6}$$

where I_o is the zeroth order modified Bessel function of the first kind. For the i^{th} envelope detector, the probability density function is given by

$$p(U_i|S_i) = U_i \exp\{-[U_i^2/2 + E/N_o]\} I_o(U_i\{2E/N_o\}^{1/2}); \quad u_i > 0$$
$$= 0; \quad u_i < 0. \tag{7}$$

To avoid the irreversible loss of information caused by hard decisions made in the demodulator prior to final decoding, soft-decision decoding is employed. (If results for the simpler case of hard-decisioning are required, they can be obtained as well.) The maximum-likelihood decision

rule for noncoherent detection and coding, requires a metric that includes a zeroth order modified Bessel function and also the noise spectral density which must be known by the decoder. A more practical decoding metric is the energy metric, which is the square of the envelope detector output. This energy metric is the most commonly used metric for coded noncoherent MFSK systems [2, vol.I.p.211] and it approximates the optimum metric for high signal-to-noise ratio.

An effective jammer against an uncoded frequency-hopped spread spectrum system is an average-power-limited partial band jammer [7]. We consider a jammer with power J that transmits Gaussian noise with constant power spectral density over a fraction α of the system bandwidth W. We define an equivalent broadband noise spectral density

$$N_J = \frac{J}{W} \tag{8}$$

The jamming noise power spectral density over the jammed bandwidth of αW Hz is then

$$N_J' = \frac{N_J}{\alpha} \tag{9}$$

and zero for the rest of the system bandwidth.

Assume that each hop is independent of other hops and equally likely to be in any part of the total spread spectrum bandwidth. The probability of a hopped signal being jammed is α. Also, assume that during any hop interval the whole set of m NCFSK tones is either totally in the jammed band or not.

Define a binary jammer state random variable Q, where Q=1 indicates that the transmitted tone hopped into the jammed band, while Q=0 indicates that it hopped outside the jammed band.

$$P[Q=1] = \alpha$$
$$P[Q=0] = 1 - \alpha \tag{10}$$

This is the jammer state information that may be available from the receiver. In the section on simulation, we will present a receiver that attempts to generate this information.

For the purposes of our early performance analysis, we will assume that the receiver knows with certainty whether each hop is jammed or not. Possible methods for deriving this information include implementing automatic gain control in the receiver, which may be monitored to determine

whether jamming power is corrupting a given hop [2, vol.II p.97]. Another method suggested by Trumpis [30] for orthogonal noncoherent FSK is to declare a hopped signal to be jammed when more than one energy detector output goes high. When nonorthogonal FSK tone spacing is employed the Trumpis approach may not be as reliable, since nonorthogonal energy detectors will also have output. However, if $\Delta = 1/2T$, two sets of orthogonal tones are obtained, in which case, there is always at least one other tone orthogonal to each transmitted tone. A hopped signal is declared to be jammed when two or more orthogonal energy detectors have high output.

The metric considered in the analysis is the suboptimum energy metric with perfect side information [2, Vol.I, p.216]. For an input X and channel output Y, it is given by

$$m(Y,X;Q) = c(Q)\, e_X \tag{11}$$

where c(Q) is a weighting function depending on the jammer state variable Q. For example, the function can simply take on one value for Q=0 and another value for Q=1. $e_X = U_X^2$ is the energy detector output (or the square of the envelope detector) corresponding to input X. The analysis includes the case of transmission in additive white Gaussian noise or full-band jamming. However, for the trellis coding of nonorthogonal signals, new theoretical results must be obtained, as previous work [2, Vol.I, p.216] has been for convolutional codes with orthogonal signalling. Simulation results will include other metrics.

III. PERFORMANCE ANALYSIS

For trellis-coded coherent multilevel and multiphase modulations, the error performance at high signal-to-noise ratio is specified by the minimum Euclidean distance between any pair of paths through the trellis. An asymptotic coding gain is usually defined as the ratio of the minimum Euclidean distance of the trellis code to the minimum distance between signals in the uncoded situation [18,20,23]. For the trellis-coded noncoherent FSK modulation with a soft energy metric and the decision rule considered here, the union Chernoff bound on bit error probability is evaluated.

Although there are situations where the Chernoff bound may not be particularly tight, it has the advantage of being relatively easy to compute and of decoupling the channel influence from the code itself [9]. Our later simulation results will indicate the bounds tend to fall within a dB of the performance at moderate signal-to-noise ratios. The Chernoff bound is widely used to obtain an upper bound on error probabilities for convolutional codes and block error-correcting codes with a maximum metric decoder (eg. a Viterbi decoder) using an arbitrary metric. This method has been shown to provide useful and reliable information [31]. Usual coded systems use orthogonal signals and the Chernoff bound on the pairwise error probability then depends on only one parameter. When nonorthogonal signals are employed, we will see that the Chernoff bound will depend on a number of parameters with each parameter corresponding to a pair of signals with a different cross-correlation coefficient.

3.1 Chernoff Bound on Pairwise Error Probability

Let $\underline{X} = (X_1, X_2, \ldots, X_N)$ be the transmitted code sequence of length N. The channel output sequence is denoted by $\underline{Y} = (Y_1, Y_2, \ldots, Y_N)$. In addition, a corresponding jammer state information sequence is denoted by $\underline{Q} = (Q_1, Q_2, \ldots, Q_N)$.

The metric used for decoding is denoted by $m(\underline{Y}, \underline{X}; \underline{Q})$. The maximum metric decoder chooses $\hat{\underline{X}} = (\hat{X}_1, \hat{X}_2, \ldots, \hat{X}_N)$ which corresponds to the maximum metric among all possible coded sequences. Error occurs whenever $\hat{\underline{X}} \neq \underline{X}$ with probability given by

$$P(\underline{X} \to \hat{\underline{X}}) = \Pr \{ \sum_{n=1}^{N} m(Y_n, \hat{X}_n; Q_n) \geq \sum_{n=1}^{N} m(Y_n, X_n; Q_n) \mid \underline{X} \}$$

$$= \Pr \{ \sum_{n=1}^{N} [m(Y_n, \hat{X}_n; Q_n) - m(Y_n, X_n; Q_n)] \geq 0 \mid \underline{X} \}$$

The pairwise error probability for this symbol-by-symbol noncoherent detection with soft decision metric decoding, cannot be evaluated except for the case when all the m NCFSK signals are orthogonal. Consequently, we have to resort to the Chernoff bound [2, Vol.I, App. 4A] on the pairwise

error probability, as commonly utilized in performance analysis of coded systems.

Applying the Chernoff bound [2, Vol.I, App. 4A], we have

$$P(\underline{X} \to \hat{\underline{X}}) \le E\left\{\exp\left(\lambda \sum_{n=1}^{N} [m(Y_n,\hat{X}_n;Q_n) - m(Y_n,X_n;Q_n)]\right) \mid \underline{X}\right\}$$

$$= E\left\{\prod_{n=1}^{M} \exp\left(\lambda\,[m(Y_n,\hat{X}_n;Q_n) - m(Y_n,X_n;Q_n)]\right) \mid \underline{X}\right\}$$

$$= \prod_{n=1}^{M} E\left\{\exp\left(\lambda\,[m(Y_n,\hat{X}_n;Q_n) - m(Y_n,X_n;Q_n)]\right) \mid \underline{X}\right\} \tag{12}$$

for any $\lambda \ge 0$.

For $\hat{X}_n = X_n$ it is clear that

$$E\left\{\exp\left(\lambda\,[m(Y_n,\hat{X}_n;Q_n) - m(Y_n,X_n;Q_n)]\right) \mid \underline{X}\right\} = 1$$

For $\hat{X}_n \neq X_n$ the expected value depends on both $\hat{X}_n$ and X_n when nonorthogonal signals are employed.

Let $\hat{X}_n = j$ and $X_n = i$, and let ρ be the crosscorrelation coefficient of the corresponding signals S_j and S_i.

For the energy metric given by (11) we have

$$D(\alpha,\lambda,\rho) = E\left\{e^{\lambda[m(Y_n,\hat{X}_n;Q_n) - m(Y_n,X_n;Q_n)]}\Big|_{\underline{X}}\right\} \hat{X}_n \neq X_n$$

$$= E\left\{e^{\lambda c(Q_n)[e_j - e_i]}\Big|_{i}\right\} \; j \neq i$$

$$= \alpha\, E\{e^{\lambda c(1)[e_j - e_i]}\Big|_{i,\,Q=1}\} + (1-\alpha)\, E\{e^{\lambda c(0)[e_j - e_i]}\Big|_{i,\,Q=0}\} \quad j \neq i \tag{13}$$

$$= \alpha\, D'(\lambda,\rho,q=1) + (1-\alpha)\, D'(\lambda,\rho,q=0) \tag{14}$$

where $$D'(\lambda,\rho,q) = E\left\{e^{\lambda c(q)[e_j - e_i]}\Big|_{i,\,Q=q}\right\} \; j \neq i \tag{15}$$

$D'(\lambda,\rho,q)$ is evaluated in Appendix A.

We wish to evaluate the performance of the noncoherent trellis codes in the following three cases:

1. additive white Gaussian noise or full-band noise jamming,
2. partial band noise jamming with jammer side information,
3. partial band noise jamming without jamming information.

For performance in additive white Gaussian noise or full band jamming set $\alpha = 1$ in (14), in which case the second term vanishes.

For partial band jamming when perfect side information is available, the metric can be chosen with c(0) large enough so that the second term in the (13) is negligible and c(1) = 1/2 chosen for normalization [2, Vol.I, p.216]. Then $D(\alpha,\lambda,\rho)$ becomes

$$D(\alpha,\lambda,\rho) = \alpha\, D'(\lambda,\rho,1)\Big|_{c(1)=1/2} \tag{16}$$

for $0 \leq \lambda < 1$.

For the case of partial band noise jamming without jamming information, c(1) = c(0) =1/2. Then the first term in (13) is given by (16). For the expected value when Q=0, that is the signal is not jammed, in (15) we simply have $e_j = |\rho|^2 E$ and $e_i = E$ when thermal background noise is neglected. Hence,

$$E\left\{e^{\lambda c(0)\,[e_j - e_i]}\Big|_i\ ,\ Q=0\right\}_{j \neq i}$$

$$= E\left\{e^{\lambda c(0)[|\rho|^2 E - E]}\right\} \tag{17}$$

For m-ary NCFSK with uniform tone spacing of Δ Hz, there are (m-1) different frequency separations between the various pairs of tones. When orthogonal tone spacing is used (Δ is an integer multiple of 1/T) $|\rho| = 0$ for all tone pairs. There is only one parameter $D(\alpha,\lambda)$ for orthogonal signaling. When nonorthogonal tone spacing is employed there are (m-1) different values of $|\rho|$ resulting in (m-1) different $D(\alpha,\lambda,\rho)$. Define

$$D_k(\alpha) = \min_{0 \leq \lambda < 1} D(\alpha,\lambda,\rho_k) \tag{18}$$

where

$$|\rho_k| = \left| \frac{\sin \pi T k \Delta}{\pi T k \Delta} \right| \tag{19}$$

The Chernoff bound on pairwise error probability can be rewritten as

$$\rho(\underline{X} \to \hat{\underline{X}}) \leq \prod_{k=1}^{m-1} [D_k(\alpha)]^{W_k(\underline{X},\hat{\underline{X}})} \tag{20}$$

where $W_k(\underline{X},\hat{\underline{X}})$ is the number of places where $|\hat{X}_n - X_n| = k \neq 0$, $n = 1,2,..,N$.

3.2 Union Chernoff Bound

These pairwise error probabilities are the basis of bit error bounds for our trellis-coded NCFSK systems. A union bound is used to upper bound all the error events that can occur. Let $a(\underline{X},\hat{\underline{X}})$ denote the number of bit errors occurring when $\underline{X}$ is transmitted and $\hat{\underline{X}}$ is chosen by the receiver. If $p(\underline{X})$ is the probability of transmitting $\underline{X}$, then the coded bit error bound has the form

$$\begin{aligned} p_b &\leq \sum_{\underline{X}} \sum_{\hat{\underline{X}} \in \zeta} a(\underline{X},\hat{\underline{X}})\, p(\underline{X})\, p(\underline{X} \to \hat{\underline{X}}) \\ &\leq \sum_{\underline{X}} \sum_{\hat{\underline{X}} \in \zeta} a(\underline{X},\hat{\underline{X}})\, p(\underline{X}) \prod_{k=1}^{m-1} [D_k(\alpha)]^{W_k(\underline{X},\hat{\underline{X}})} \end{aligned} \tag{21}$$

where ζ is the set of all coded sequences.

An efficient method for evaluating the union bound is the transfer function technique [25, 27]. Since the output of the trellis encoder is determined by the input bit sequence and the state of the trellis encoder, a state diagram is a more compact representation of the code than the trellis diagram. For the performance evaluation of our trellis-coded NCFSK, the state transition branches are labeled with $L^{\ell} I^{i} D_k$. L and I are just dummy variables and D_k denotes the parameter given by (18) when the incorrect and correct channel signals associated with the state transition are separated by $k\Delta$ Hz. The exponents ℓ and i denote the number of channel symbols and the bit error corresponding to the state transition.

Let $\underline{D}$ denote the (m-1)-tuple of $D_k(\alpha)$ given by (18). The transfer function denoted by $T(L,I,\underline{D})$ derived from the state diagram, enumerates all possible pairwise error probabilities in a closed form.

For trellis codes which are in general nonlinear, the probability of error for deciding an incorrect path is dependent on the correct path. Consequently, one cannot assume the all-zeros code sequence to be the transmitted code sequence, as is usually done for linear codes. Biglieri's method [26] of pairwise states or product states involves a generalized state diagram defined over an expanded set of product states. The generalized transfer function so derived enumerates all possible incorrect paths for all possible correct paths. For an η-state trellis this method requires a product state diagram of η^2 states or equivalently a $\eta^2 x \eta^2$ state transition matrix for computing the transfer function. Consequently, this method is useful for trellis codes with only a small number of states.

Another method suitable for trellis codes having certain symmetries such as the Ungerboeck codes and other codes based on set partitioning, has been derived by Zehavi and Wolf [27]. This method requires a modified state diagram consisting of η states for a η-state trellis code. It is therefore more computationally efficient than the product state method and is employed here.

The union Chernoff bound on bit error probability is then given by

$$p_b \leq \frac{1}{2} \frac{1}{k} \frac{\partial}{\partial I} T(L,I,\underline{D}) \Big|_{\substack{L=2^{-k} \\ I=1}} \tag{22}$$

with a factor of 1/2 added to improve the Chernoff bound [2, Vol.I. App.4B]. The worst case partial band noise jamming performance is then obtained by maximizing p_b over $0<\alpha\leq 1$ as

$$p_{b\ WC} \leq \max_{0<\alpha\leq 1} \frac{1}{2} \frac{1}{k} \frac{\partial}{\partial I} T(L,I,\underline{D}) \Big|_{\substack{L=2^{-k} \\ I=1}} \tag{23}$$

It should be noted that the maximizing value of α is not necessarily equal to the worst case α, because a bound rather than an equality is maximized.

3.3 Transfer Functions of the Specific Codes

In this section the particular trellis codes investigated, and their transfer functions are presented. It was decided to focus investigation on 4-ary noncoherent frequency-shift-keying as the modulation format. Trellis coding with 2-state, 4-state and 8-state trellises have been studied. Nonorthogonal NCFSK tone spacing of 1/3T, 1/2T and 2/3T have been

considered together with orthogonal spacing of 1/T. Union Chernoff bounds on bit error probability were found when the system is under thermal noise (full band jamming) and worst case partial band noise jamming, using the theory outlined above.

3.3.1 4-NCFSK with 2-state trellis coding

The binary input sequence is coded into a 4-NCFSK signal by a rate 1/2 2-state trellis encoder. Fig. 3 depicts the signal set partitioning, the signal assignments to the state transitions and the modified state diagram. From the state diagram the following state equations are obtained.

$$T(L,I,\underline{D}) = 2\,L\,D_1\,\chi_1 \tag{28}$$

$$\chi_1 = L\,I\,(D_1+D_3)\,\chi_1 + 2\,L\,I\,D_2 \tag{29}$$

Solving (28) and (29), we obtain the transfer function given by

$$T(L,I,\underline{D}) = \frac{4L^2\,ID_1D_2}{1-L\,I(D_1+D_3)} \tag{30}$$

for this 2-state trellis coding.

3.3.2 4-NCFSK with 4-state trellis coding

The set partitioning of the 4-ary NCFSK signals remains the same as for 2-state trellis coding. With a 4-state trellis, there are more state transition branches and Ungerboeck's rules 2) and 3) given in [19] can now be simultaneously satisfied. The signal set partitioning, assignment of signals to transition branches and the modified state diagram for this 4-state trellis coding, are shown in Fig.4.

From the state diagram, we get the following state equations

$$T(L,I,\underline{D}) = 2\,L\,D_2\chi_c \tag{31}$$

$$\chi_a = 2\,L\,I\,D_2 + 2\,L\,I\,\chi_c \tag{32}$$

$$\chi_b = L\,I\,(D_1+D_3)\,\chi_a + 2\,L\,I\,D_1\chi_b \tag{33}$$

$$\chi_c = 2\,L\,D_1\chi_a + L\,(D_1+D_3)\,\chi_b \tag{34}$$

Solving (31) to (34) yields

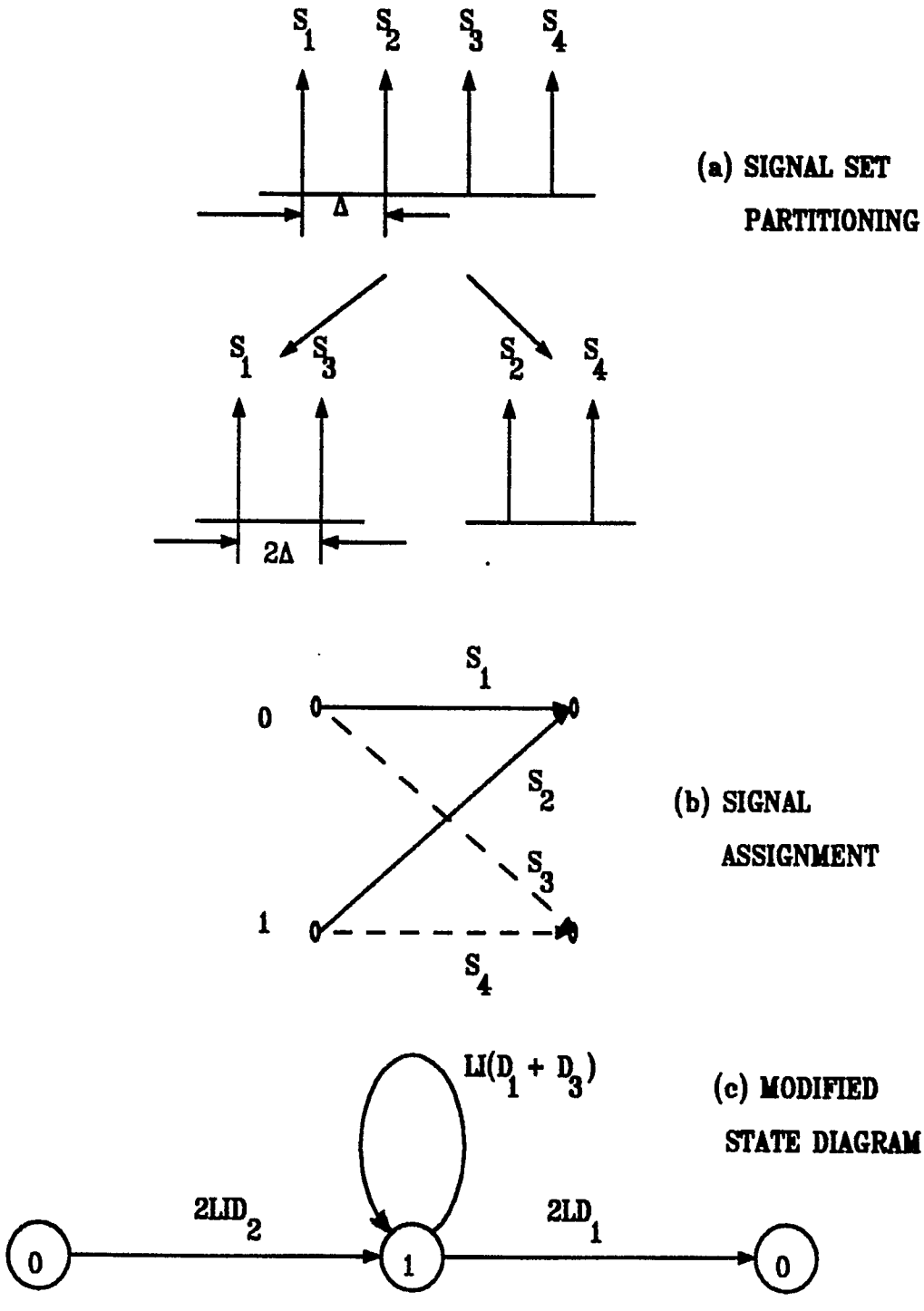

Figure 3: 4-NCFSK with 2-state trellis coding.

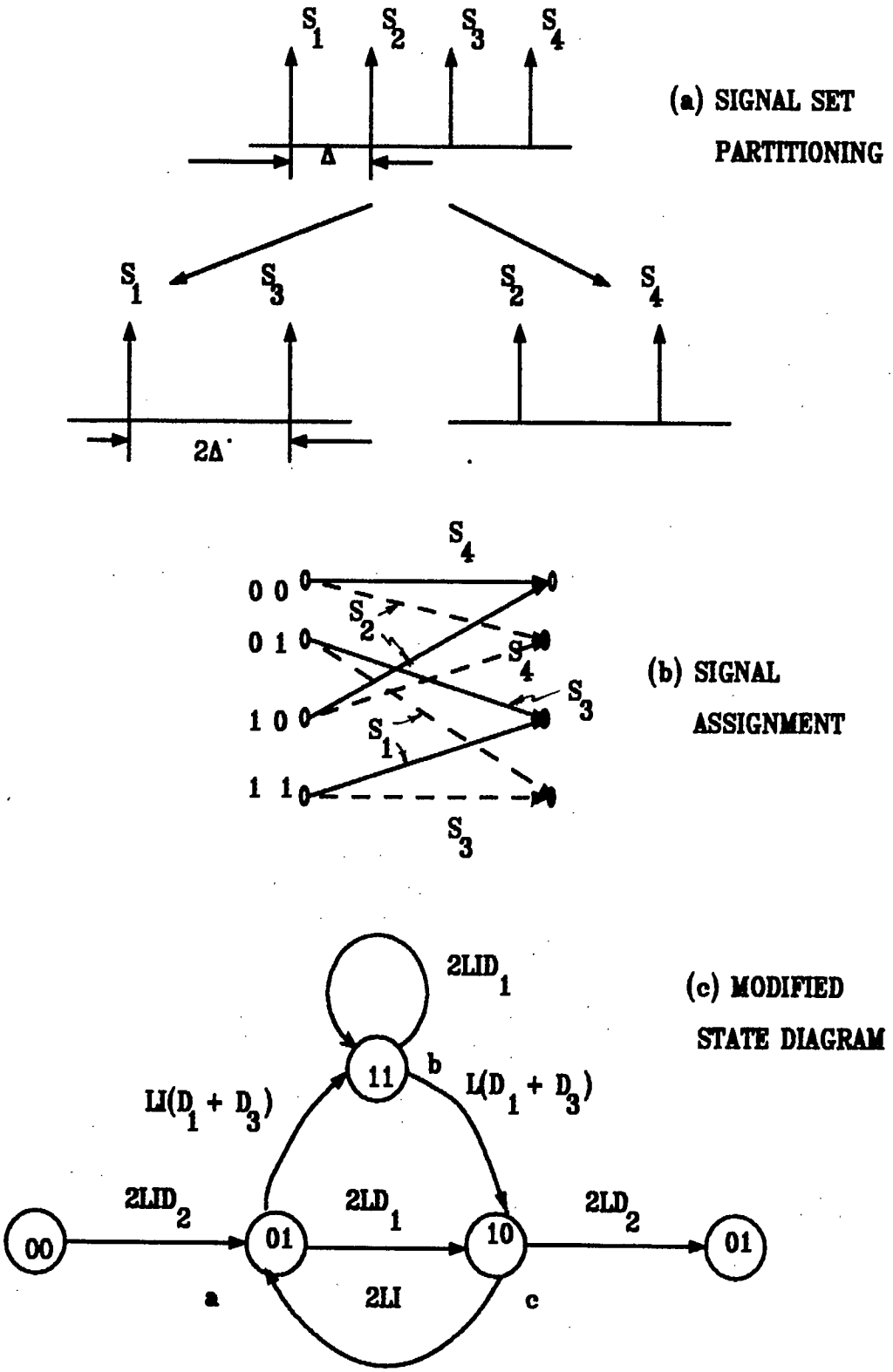

Figure 4: 4-NCFSK with 4-state trellis coding.

$$T(L,I,\underline{D}) = \frac{2\,L\,D_2[2\,L^3I^2D_2(D_1+D_3)^2 + 4\,L^2I\,D_1D_2(1-2\,L\,I\,D_1)]}{1 - 2\,L\,I\,D_1 - 2\,L^3I^2(D_1+D_3)^2 - 4\,L^2I\,D_1(1-2\,L\,I\,D_1)} \quad (35)$$

3.3.3 4-NCFSK with 8-state trellis coding

Again, the set partitioning of the 4-ary NCFSK signals remains the same as for 2 and 4-state trellis coding. With an 8-state trellis, there are even more state transition branches and equations, which will be indicated below for completeness. The signal set partitioning and the assignment of signals to transition branches are shown in Fig. 5. The modified state diagram for the 8-state trellis coding, is shown in Fig.6.

From the state diagram, we get the following state equations

$$T(L,I,\underline{D}) = 2\,L\,D_2X_4 \quad (36)$$

$$X_1 = 2\,L\,I\,D_2 + 2\,L\,I\,X_4 \quad (37)$$

$$X_2 = 2\,L\,D_1X_1 + L\,(D_1+D_3)\,X_5 \quad (38)$$

$$X_3 = L\,I\,(D_1+D_3)\,X_1 + 2\,L\,I\,D_1X_5 \quad (39)$$

$$X_4 = 2\,L\,X_2 + 2\,L\,D_2X_6 \quad (40)$$

$$X_5 = 2\,L\,I\,D_2X_2 + 2\,L\,I\,X_6 \quad (41)$$

$$X_6 = 2\,L\,D_1X_3 + L\,(D_1+D_3)\,X_7 \quad (42)$$

$$X_7 = L\,I\,(D_1+D_3)\,X_3 + 2\,L\,I\,D_1\,X_7 \quad (43)$$

Solving (36) to (43) yields

$$T(L,I,\underline{D}) = \frac{4\,L^2I\,D_2^2\,C_N}{C_D - 2\,L\,I\,C_N} \quad (44)$$

where $C_D = A_D\,B_D$ (45)

$$C_N = 4L^2D_1A_DB_D + 2L^2(D_1+D_3)A_DB_N + 2L^2ID_2(D_1+D_3)A_NB_D + 4L^2ID_1D_2A_NB_N \quad (46)$$

$$B_N = 4L^2ID_1D_2A_D + 2L^2I^2(D_1+D_3)A_N \quad (47)$$

$$B_D = [1 - 2L^2ID_2(D_1+D_3)]A_D - 4L^2I^2D_1A_N \quad (48)$$

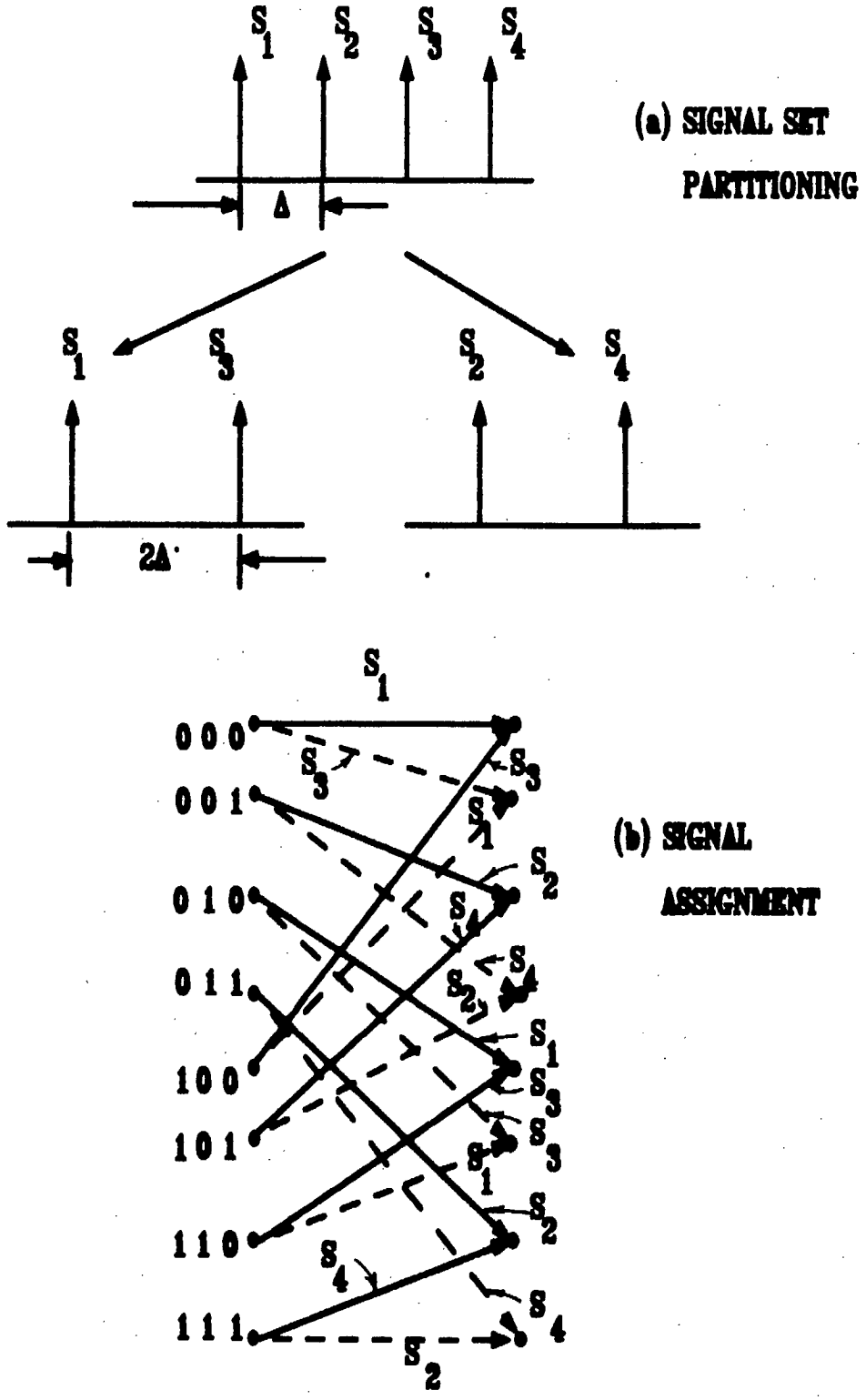

Fig. 5. 4-NCFSK with 8-state trellis coding. Signal Set.

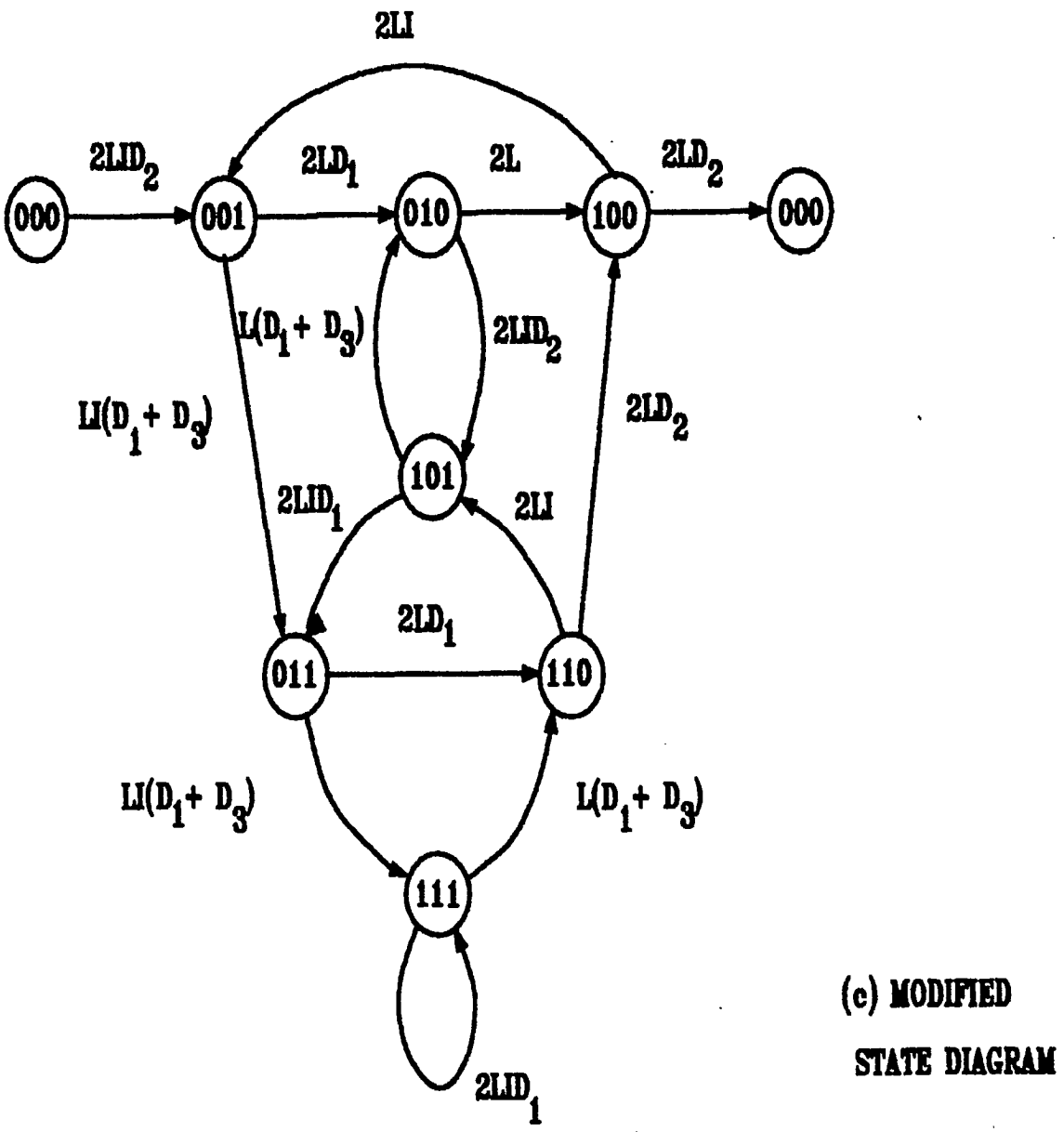

Fig. 6. 4-NCFSK with 8-state trellis coding. State Diagram.

$$A_N = 2LD_1 - 4L^2ID_1^2 + L^2I(D_1 + D_3)^2 \quad (49)$$

$$A_D = 1 - 2\,L\,I\,D_1 \quad (50)$$

IV. SYSTEM PERFORMANCE EVALUATION

In this section the performance of frequency-hopped trellis-coded 4-ary noncoherent frequency-shift-keying is evaluated. A 4-ary modulation was chosen to keep the initial computations relatively simple and to keep simulation times short, hopefully. Preliminary consideration of higher order modulations such as 8-ary NCFSK, lead us to anticipate similar performance improvements. Trellis coding with 2-state, 4-state and 8-state trellises have been investigated. Nonorthogonal NCFSK tone spacing of 1/3T, 1/2T and 2/3T have been considered together with orthogonal spacing of 1/T. Union Chernoff bounds on bit error probability have been computed using the theory presented above and the results compared with the simulations. Performance has been evaluated in which the system is in thermal noise or full-band jamming, and has been evaluated for worst case partial band noise jamming. Results are presented for performance with and without coding, and with and without the use in the decoder of information on the jammer derived in the receiver.

4.1 Performance in Additive Noise

We first examine the performance of the coded system in additive Gaussian noise. The union Chernoff bounds on bit error probability for 4-NCFSK with 2-state trellis coding with tone spacing Δ = 1/3T, 1/2T, 2/3T and 1/T were evaluated and are plotted in Fig. 7. In the simulated system as indicated in Fig.1, the samples from the energy detectors were fed to a Viterbi decoder. The best performance is obtained when all the tones are orthogonal with Δ = 1/T, as expected.

To avoid large bandwidth expansion, the use of nonorthogonal tone spacing has been investigated. For Δ = 1/3T, the bandwidth occupancy of the coded 4-NCFSK is the same as (or slightly less than, depending on the bandwidth criterion used) that of the uncoded orthogonal binary NCFSK but the performance is worse by approximately 1 dB. As the spacing is increased the performance improves. For example, if a spacing of Δ = 1/2T is used,

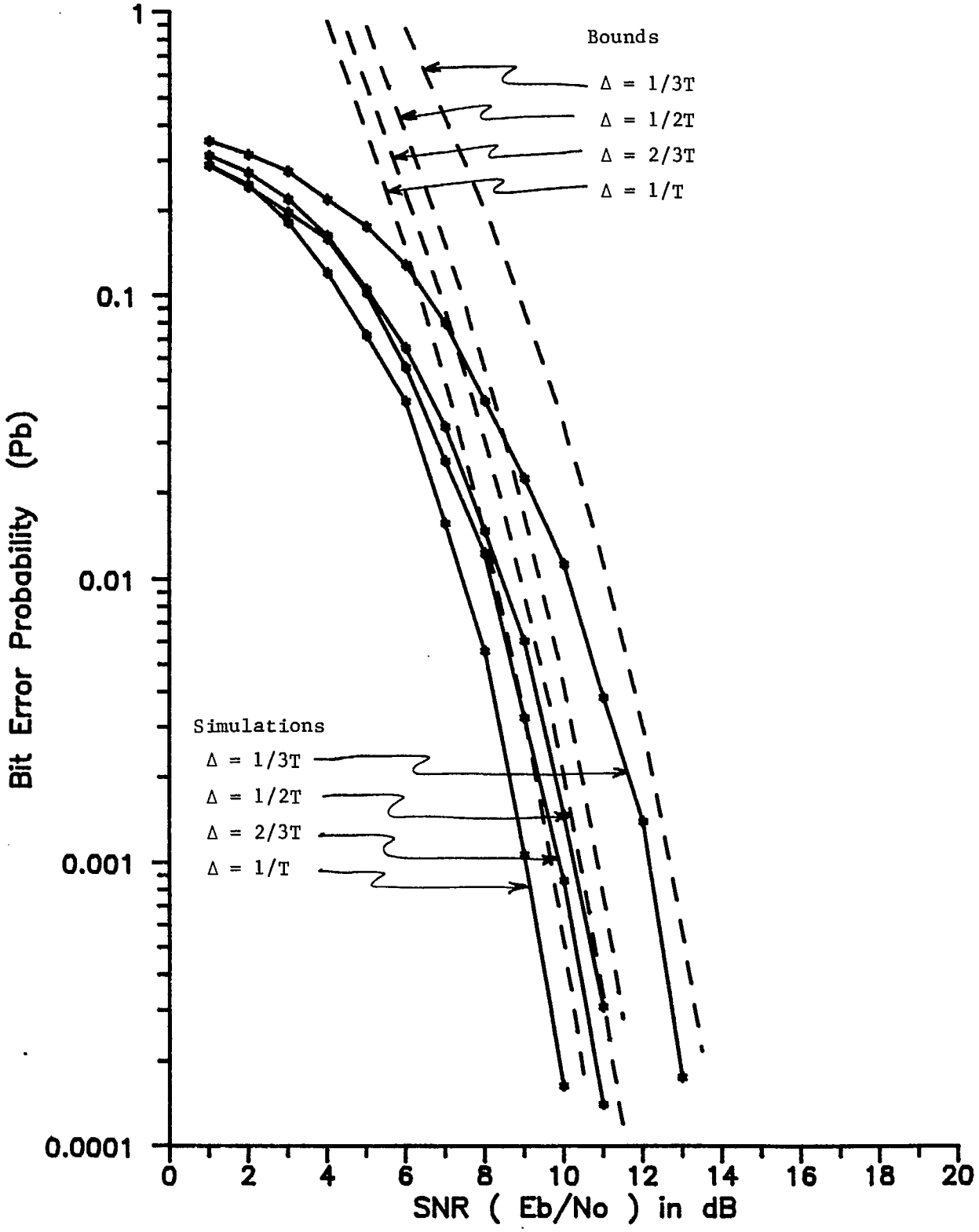

Figure 7 . Performance of 4-ary NC FSK with 2 State Trellis Coding in AWGN using soft energy metric

two sets of orthogonal tones are obtained in the trellis, and the performance is better than that of uncoded orthogonal binary NCFSK by about 3/4 dB. The orthogonal spacing of $\Delta = 1/T$ yields the best performance with an improvement over the uncoded case by 2 dB.

The simulation results indicate that the bounds predict the error performance at moderate signal to noise ratios, within a fraction of a dB.

The performance of 4-NCFSK in Gaussian noise with 4-state and 8-state trellis coding, are presented in Figs. 8 and 9. Again, results for $\Delta = 1/3T$ 1/2T and 2/3T show that the performance improves as the spacing is increased. Implementing a 4-state code brings a further improvement of from 1.5 to 2 dB., depending on the particular spacing being considered. There appears to be only a miniscule improvement in increasing from 4 to 8 states.

4.2 Performance in Partial Band Jamming

In this section, the performance of the systems in noise jamming will be considered, where the bandwidth of the noise has been selected by the jammer to give the maximum error-rate: worst-case partial band jamming. The baseline performance of uncoded binary NCFSK in worst-case partial band jamming is also plotted in Fig. 10 for reference. Figs. 11, 12 and 13 give the performance of the encoded system with a Viterbi decoder, for 2, 4 and 8-state trellis codes. The performance of the 2-state code is about 1 dB. worse than that of the uncoded system with orthogonal frequency spacing. However the 4 and 8-state trellis codes are about 2.7 dB. better than the uncoded system with orthogonal spacing. This improvement disappears at very low signal-to-jamming ratios. As well, there appears to be no significant improvement in going to an 8-state code. At the higher signal-to-jamming ratios where the trellis codes show improvement, the appears to be little degradation in using the narrower nonorthogonal signal spacings.

A very substantial improvement in performance is attainable if the receiver is able to estimate with reasonable accuracy the presence of jamming in the particular hop being received. Figs. 14, 15 and 16 indicate the performance that can be achieved if the receiver can pass to the decoder perfect information as to whether or not the hop has been jammed. Although there is improvement over binary NCFSK with the 2-state coding and perfect jammer information, the most substantial improvement comes with the 4-state

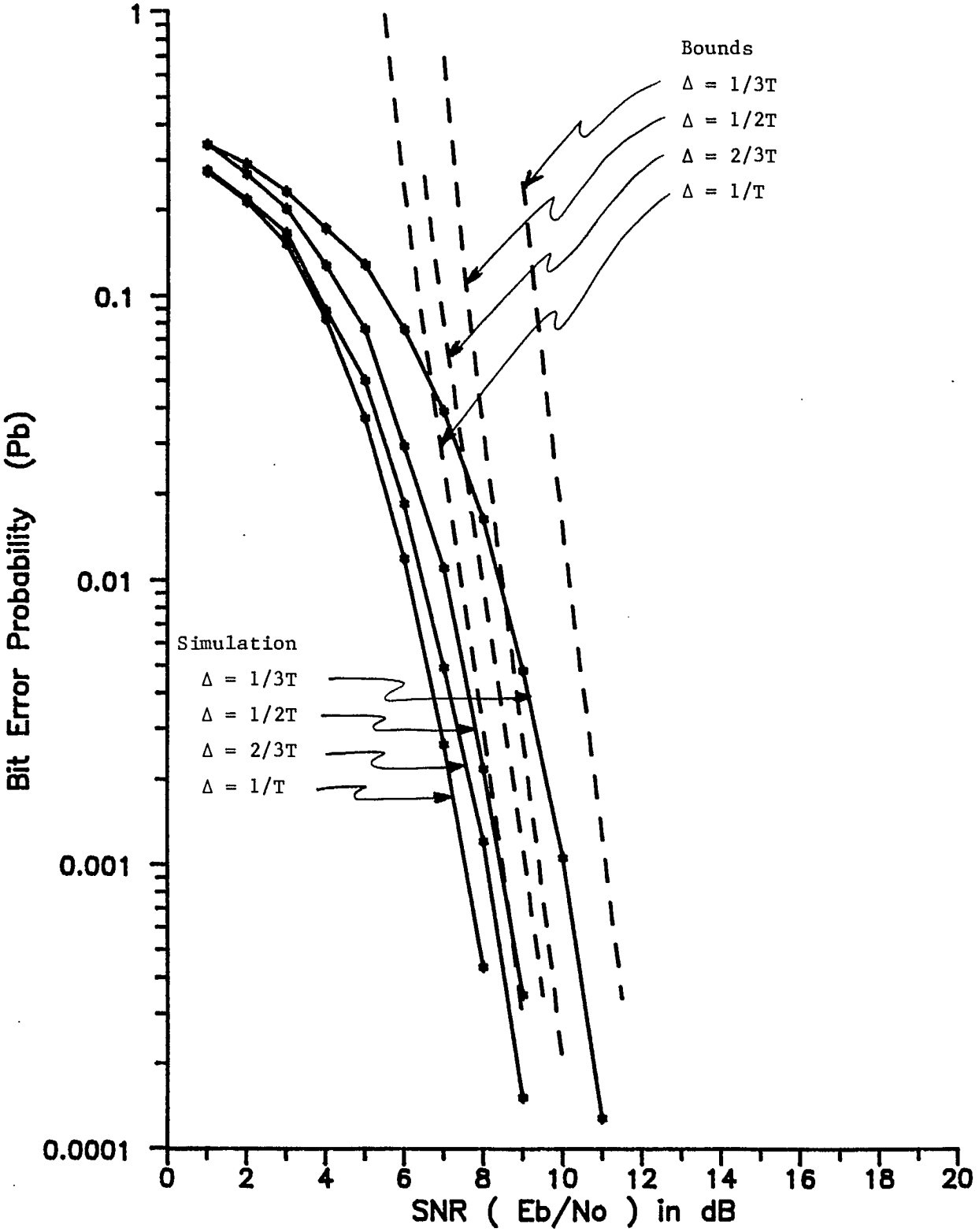

Figure 8 Performance of 4-ary NC - FSK with 4 State Trellis Coding in AWGN - soft energy metric

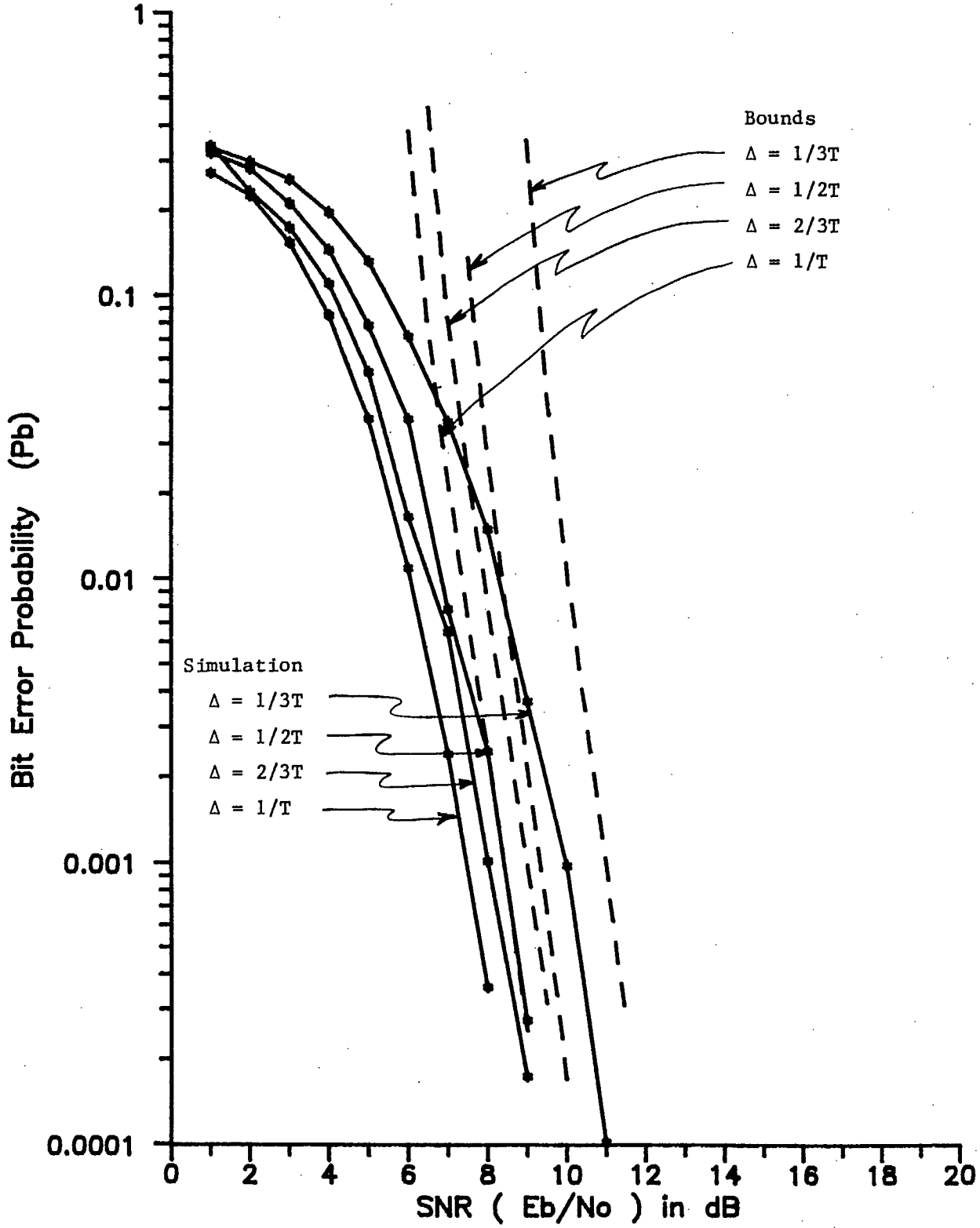

Figure 9 Performance of 4-ary NC - FSK with 8 state trellis coding in AWGN - soft energy metric

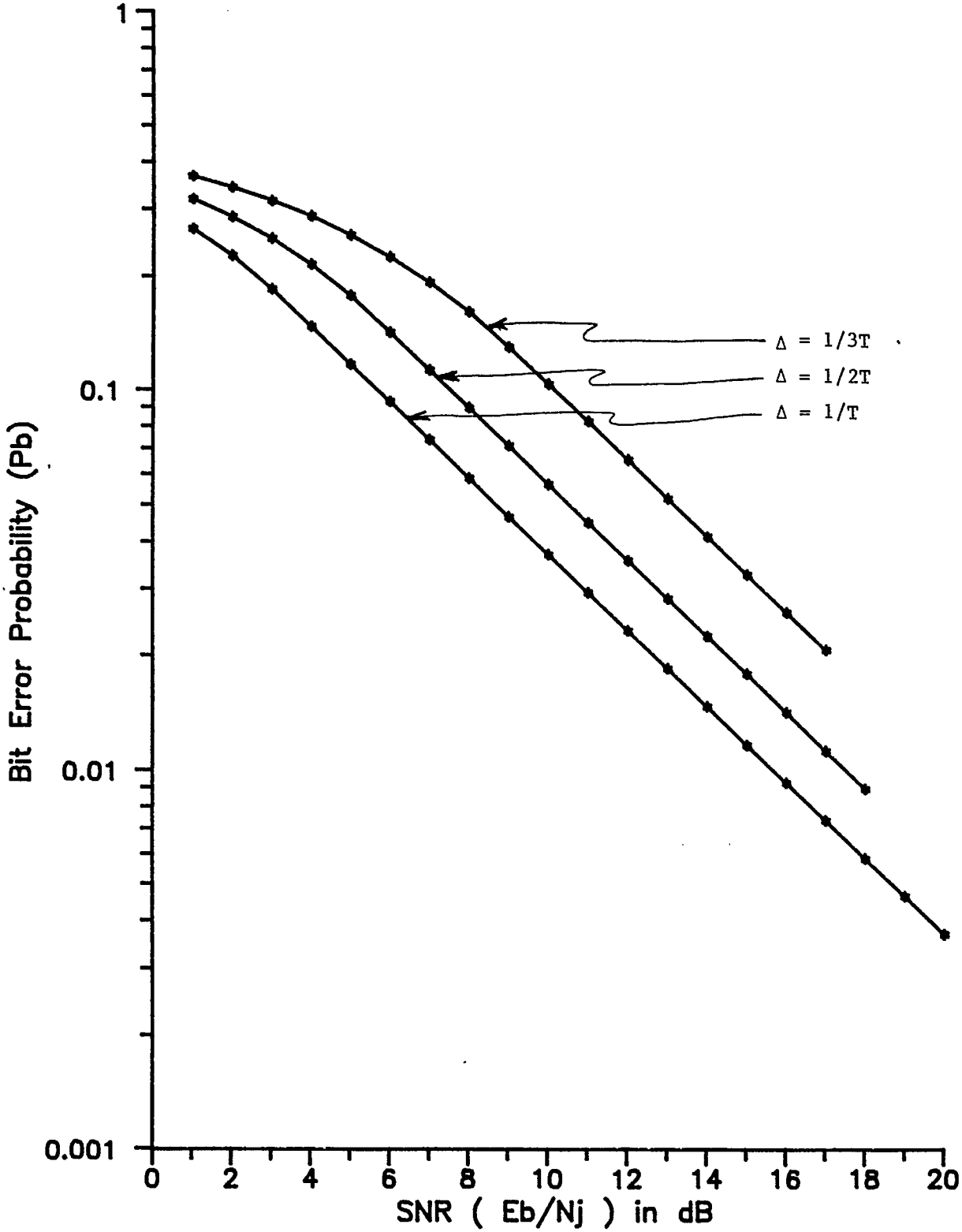

Figure 10 Performance of uncoded binary NC-FSK in worst case partial band jamming

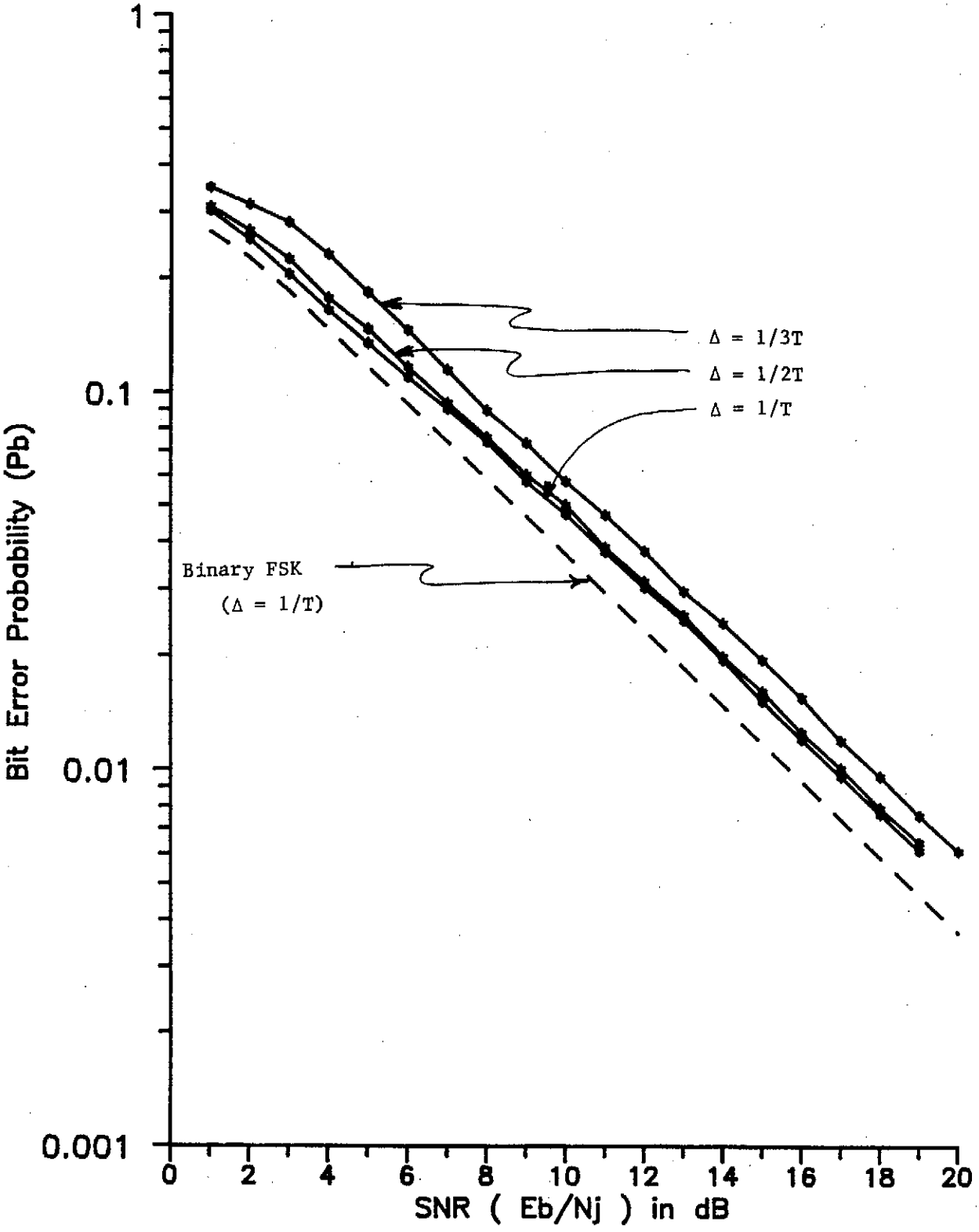

Figure 11 Performance of 4-ary NC - FSK with 2 state trellis coding in worst case partial band jamming using soft energy metric with no side information

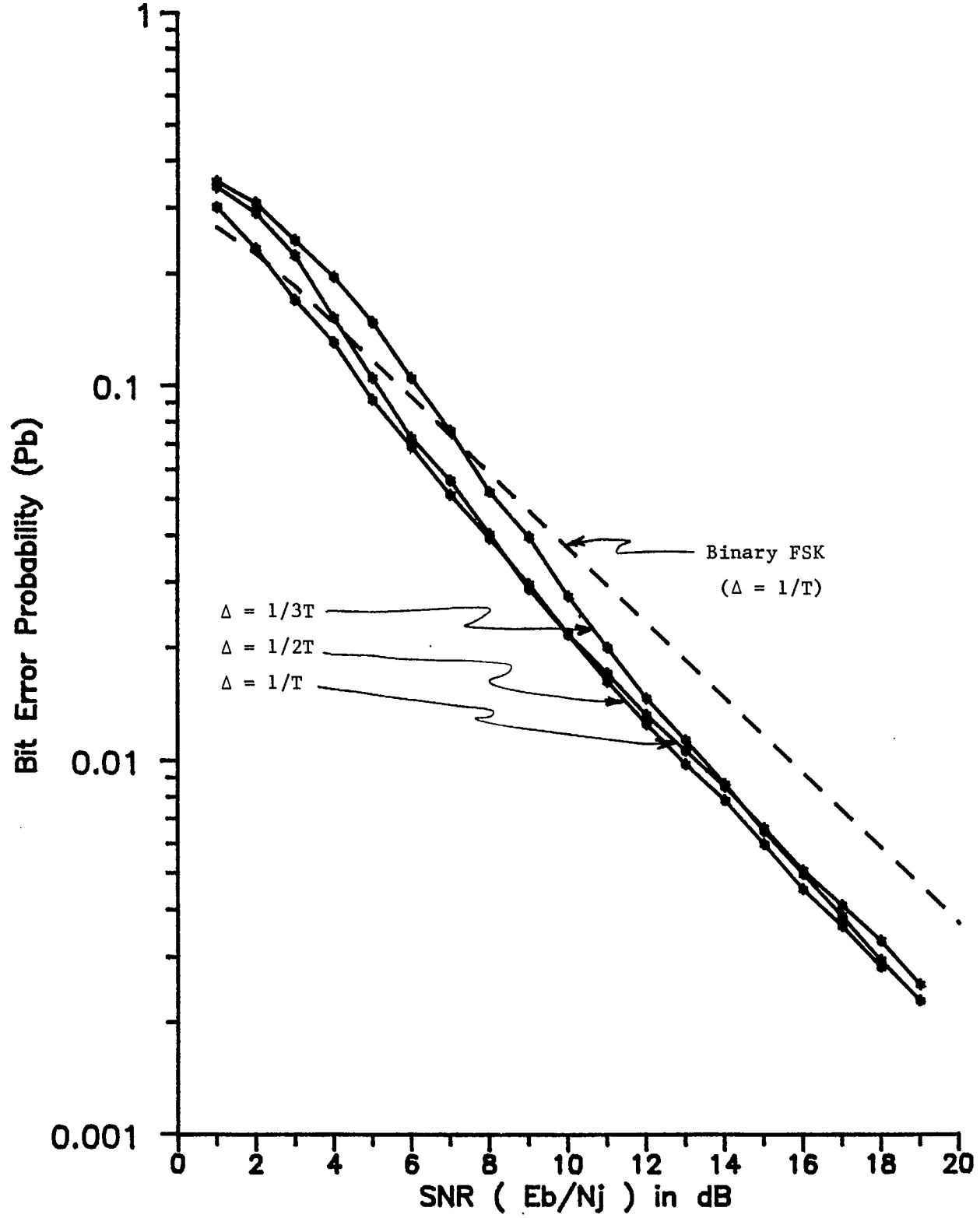

Figure 12 Performance of 4-ary NC - FSK with 4 state trellis coding in worst case partial band jamming using soft energy metric with no side information

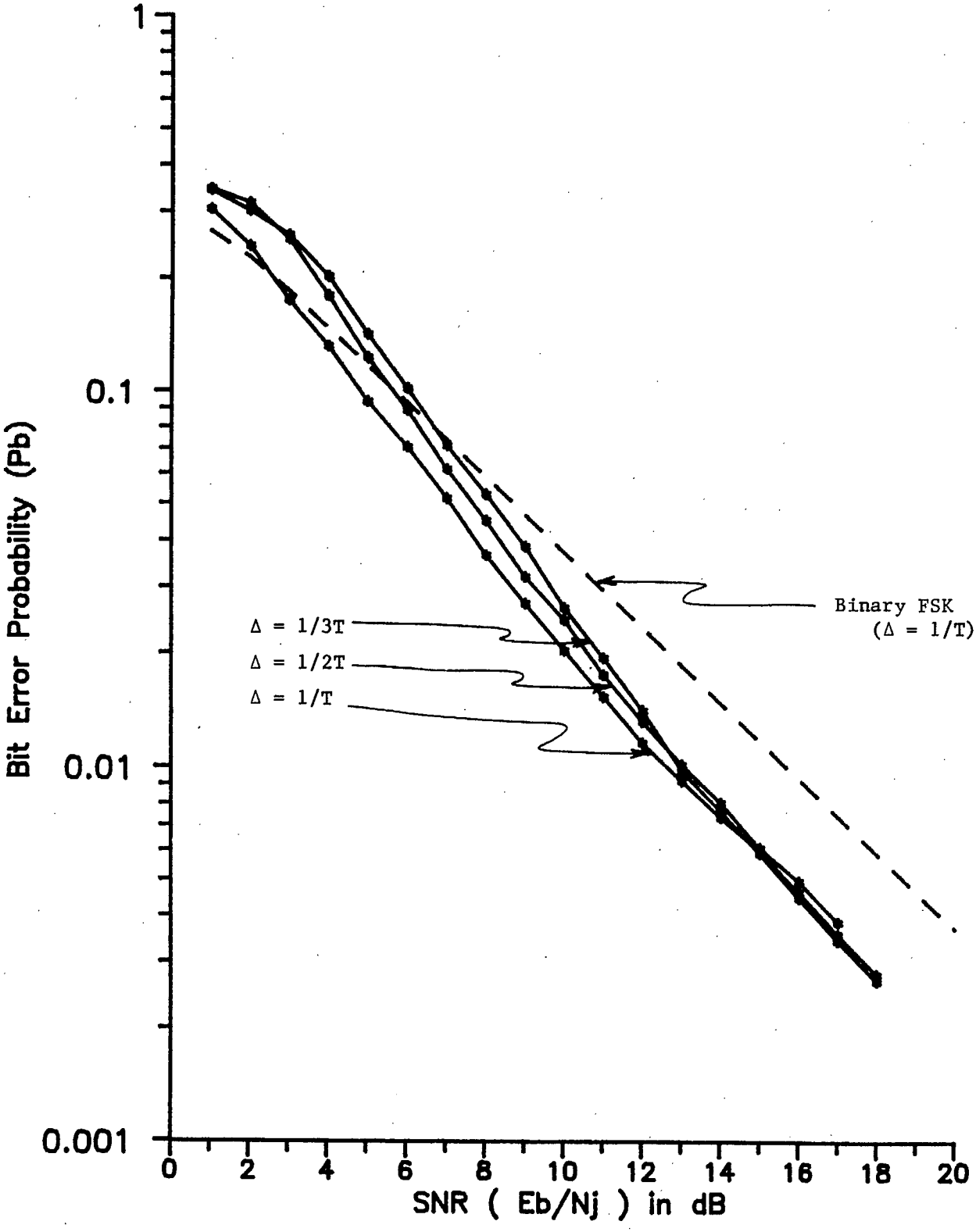

Figure 13 Performance of 4-ary NC-FSK with 8 state trellis coding in worst case partial band jamming using soft energy metric with no side information

encoding. Little additional improvement is achieved with the 8-state encoder and receiver.

At the higher signal-to-jamming ratios the improvements due to coding are very dramatic. In this region the bounds are tight and Table 1 summarizes the coded performance under worst case partial band noise jamming, by tabulating the required signal to jamming noise ratio in dB to achieve a bit error rate of 10^{-5}. The corresponding worst case fraction of the band jammed, α^*, which maximized the bit error rate is also listed. The use of nonorthogonal signals with tone spacing of 1/2T Hz rather than 1/T Hz for orthogonal signaling, increases the required signal to noise ratio by only 1/2 a dB or so.

As an additional verification of the utility of the bounds, a comparison was carried out of the worst case performance achieved with coding with perfect jammer side information, where the worst case fraction of the band jammed was calculated first using the bounds and the was determined by simulation. These results are shown in Figs. 17 to 19, for the various trellis encodings. Little difference is seen between the results obtained with the bound and with the simulations.

The results for the Viterbi detection where there is perfect information with regard to the presence of the jammer, appear extremely attractive. However the question as to how close a practical receiver might come to this performance follows naturally. Thus we simulated a receiver which weights or divides the output of each energy detector by the sum of the energies in all the detectors, prior to passing the variables to the Viterbi decoder. The results for the various state codes are shown in Figs. 20 -22. A comparison of the results for this self-normalizing metric with those for perfect side information are shown. The agreement is quite close. In some cases the performance of the self-normalizing metric appears better than that for perfect side information. However it should be borne in mind that the comparison is with perfect side information where the fraction of the band jammed has been chosen to achieve the worst possible performance when the jammer information is perfect. A different fraction would prove worse for the self-normalizing metric. As well, there are regions where the performance of the self normalizing metric changes significantly. This is

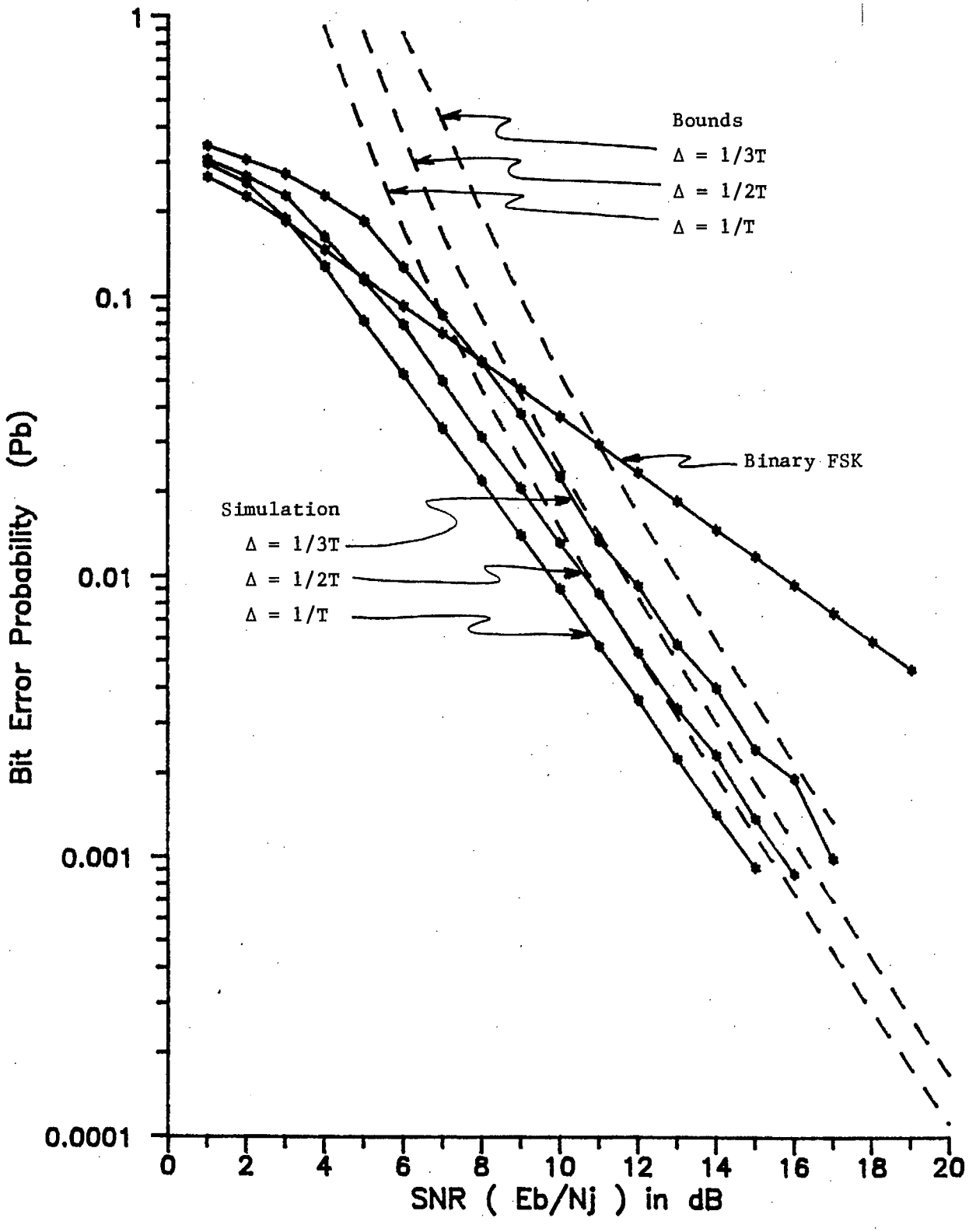

Figure 14 Performance of 4-ary NC-FSK with 2 state trellis coding in worst case partial band jamming with perfect side information. Worst case fraction determined by simulation.

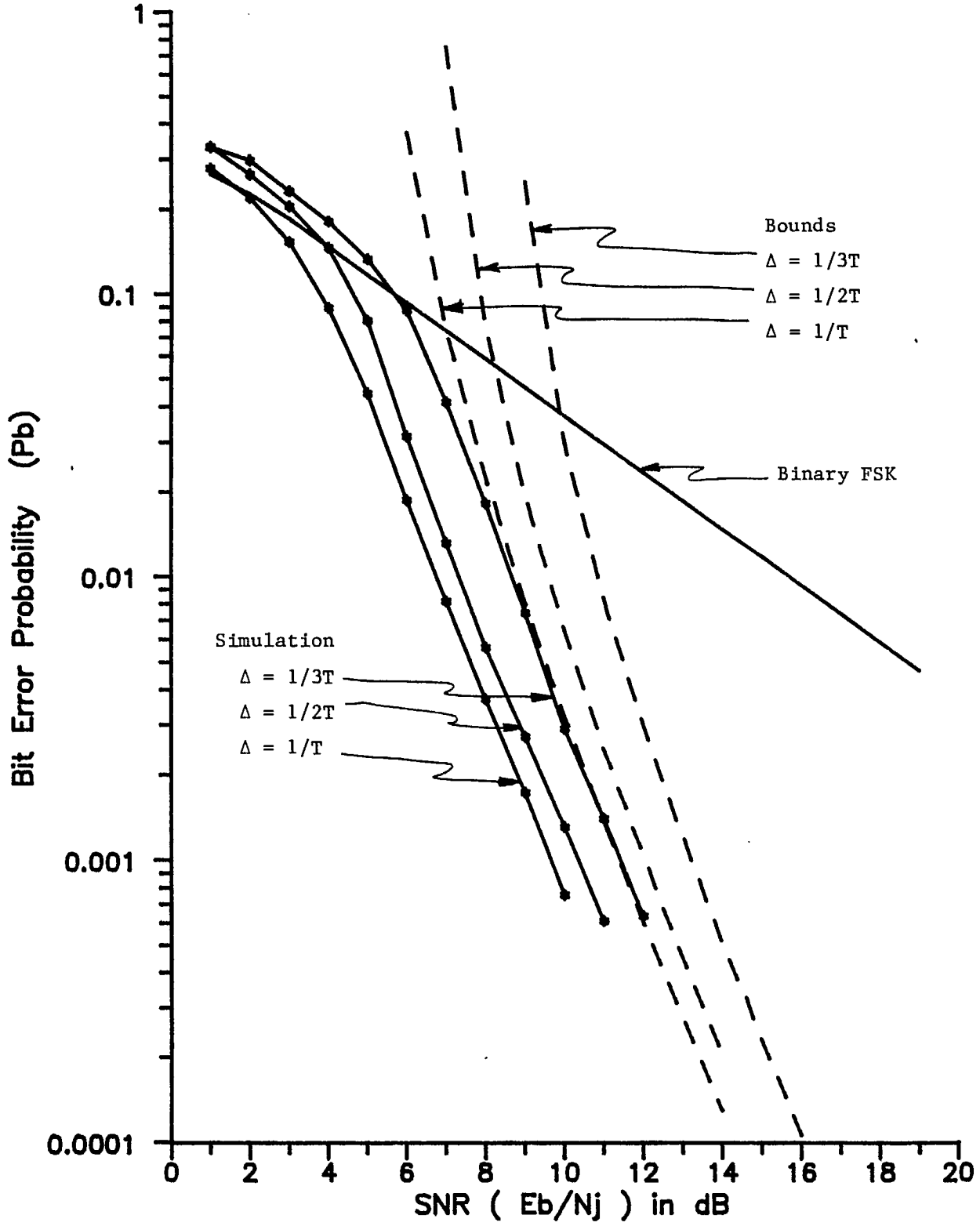

Figure 15 Performance of 4-ary NC - FSK with 4 state trellis coding in worst case partial band jamming with perfect side information. Worst case fraction determined by simulation.

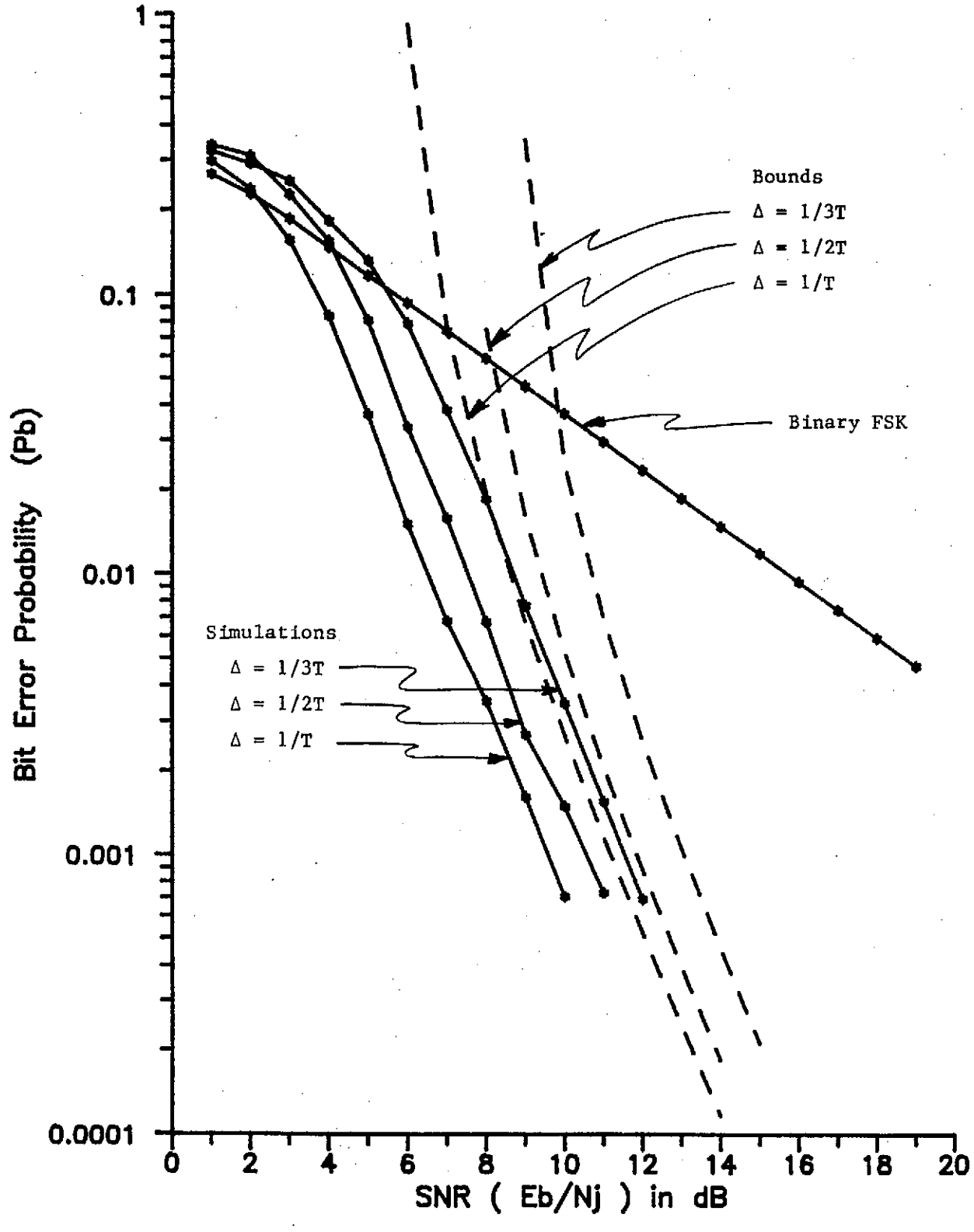

Figure 16 Performance of 4-ary NC-FSK with 8 state trellis coding in worst case partial band jamming with perfect side information. Worst case fraction determined by simulation.

	Tone Spacing	E_b/N_J in dB for $P_b < 10^{-5}$	worst case fraction of jammed band, α^*
uncoded binary NCFSK	1/T	45.66	5.44×10^{-5}
2 - state trellis code	1/3T	27	1.12×10^{-2}
	1/2T	26	9.60×10^{-3}
	1/T	25.17	9.12×10^{-3}
4 - state trellis code	1/3T	19.2	6.63×10^{-2}
	1/2T	18.0	5.56×10^{-2}
	1/T	17.50	5.34×10^{-2}

Table 1: Performance of frequency-hopped trellis-coded 4-ary noncoherent frequency-shift-keying under worst case partial band noise jamming, decoding with jammer information.

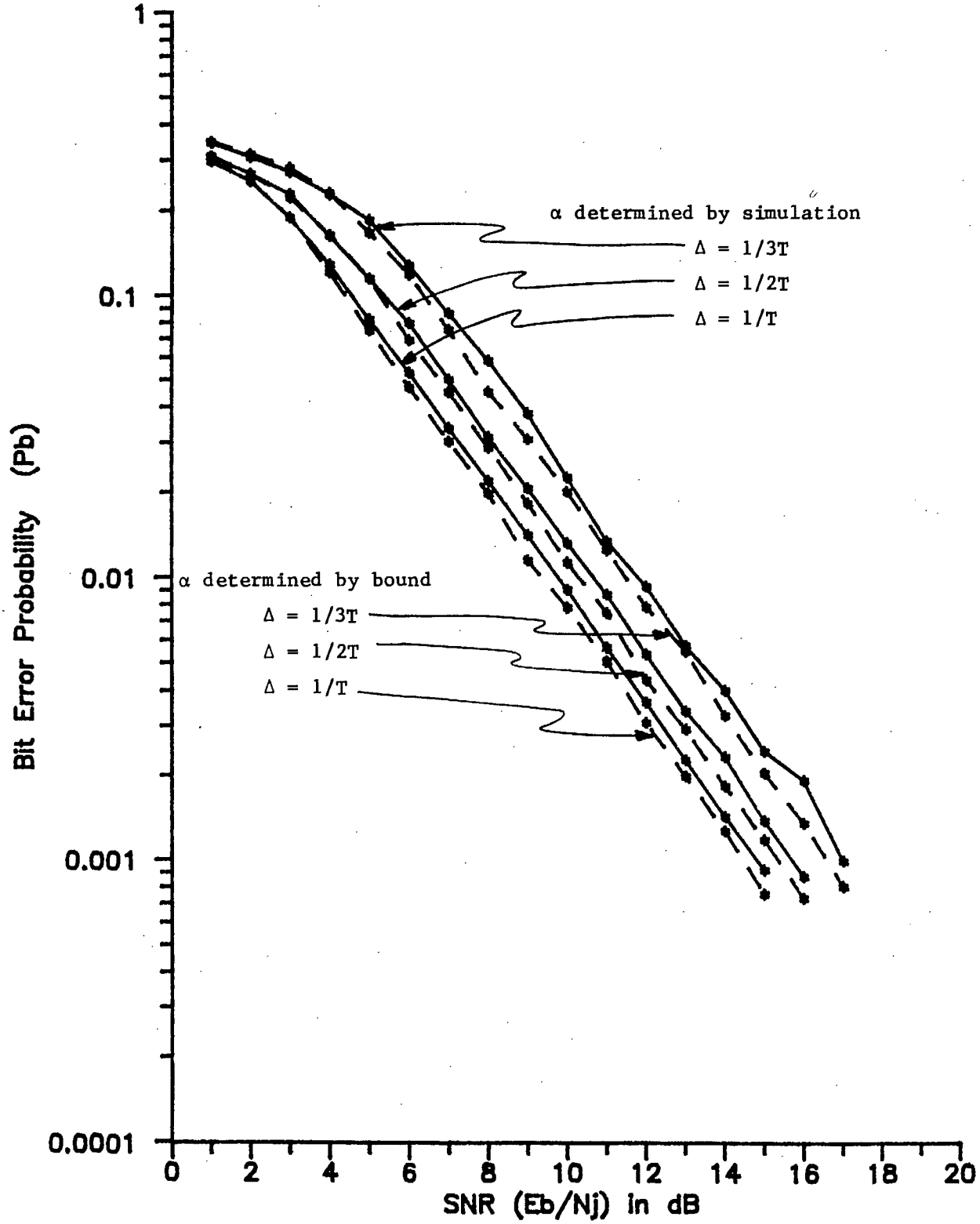

Figure 17 Performance of 4-ary NC-FSK with 2 state trellis coding in partial band jamming with perfect side information. Comparison of results where fraction of band jammed (α) is determined by simulation and by bounding.

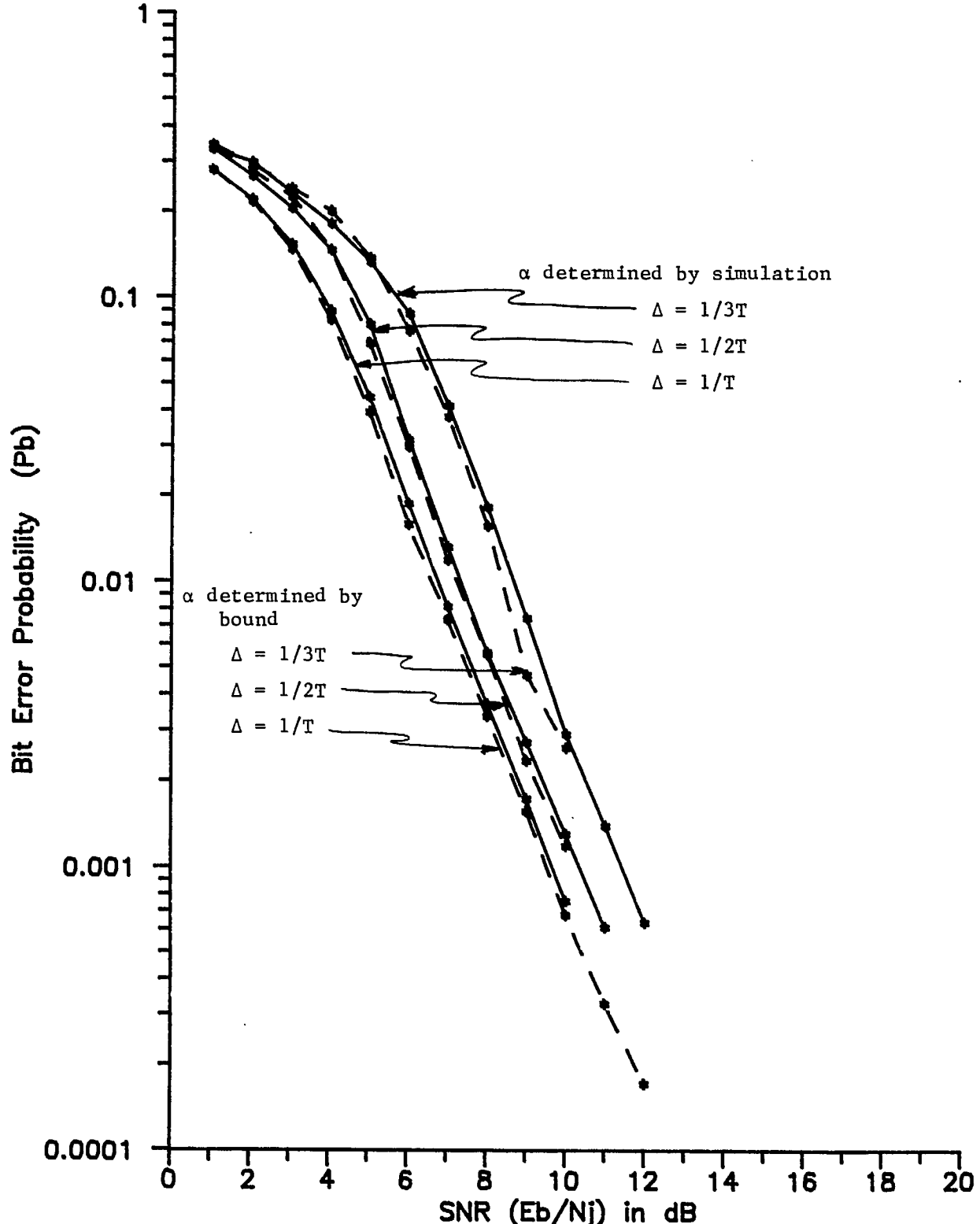

Figure 18 Performance of 4-ary NC-FSK with 4 state trellis coding in worst case partial band jamming with perfect side information. Fraction of band jammed (α) derived by simulation and by bounding.

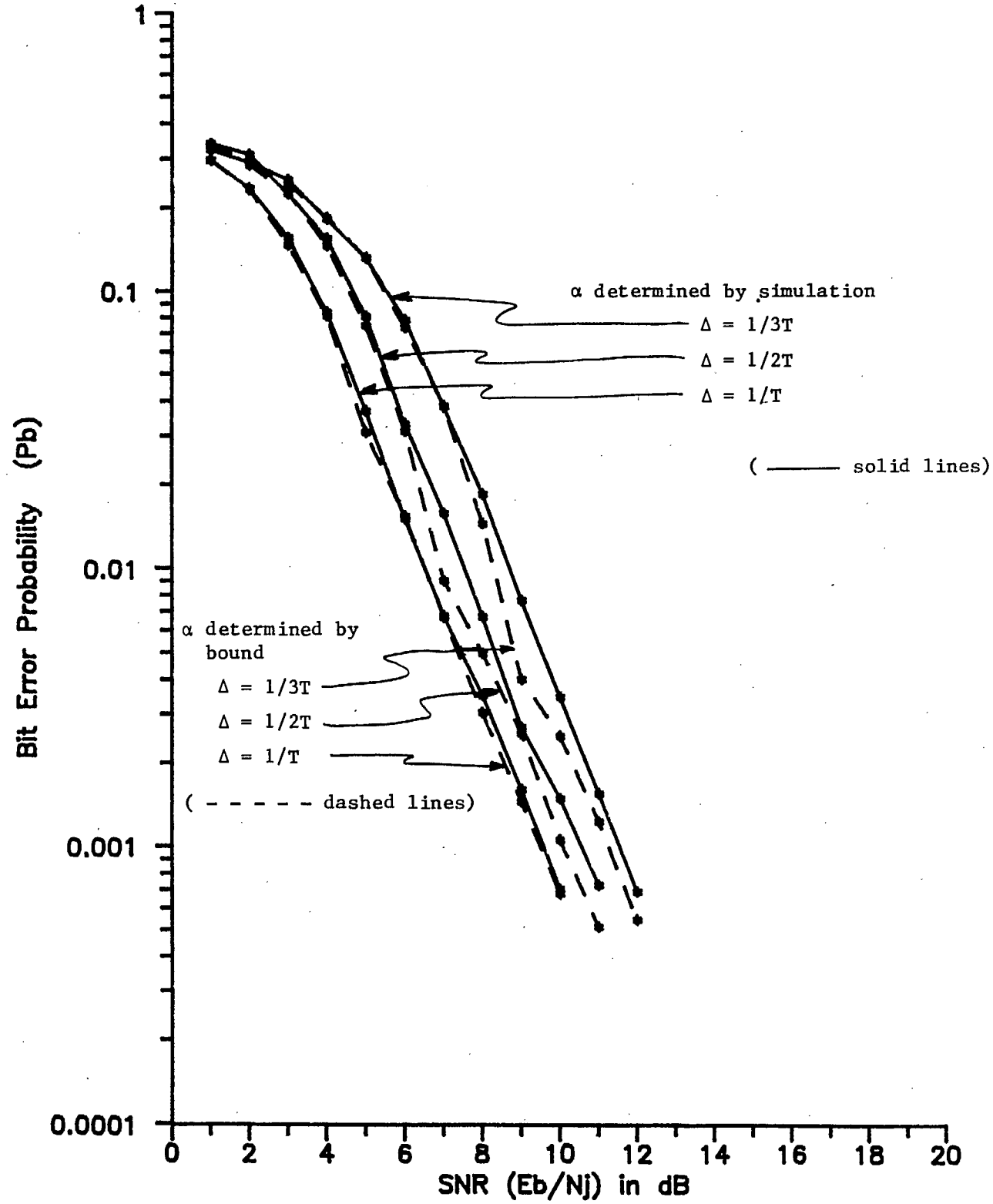

Figure 19 Performance of 4-ary NC FSK with 8 state trellis coding in worst case partial band jamming with perfect side information. The fraction of band jammed (α) determined by simulation and by bounding.

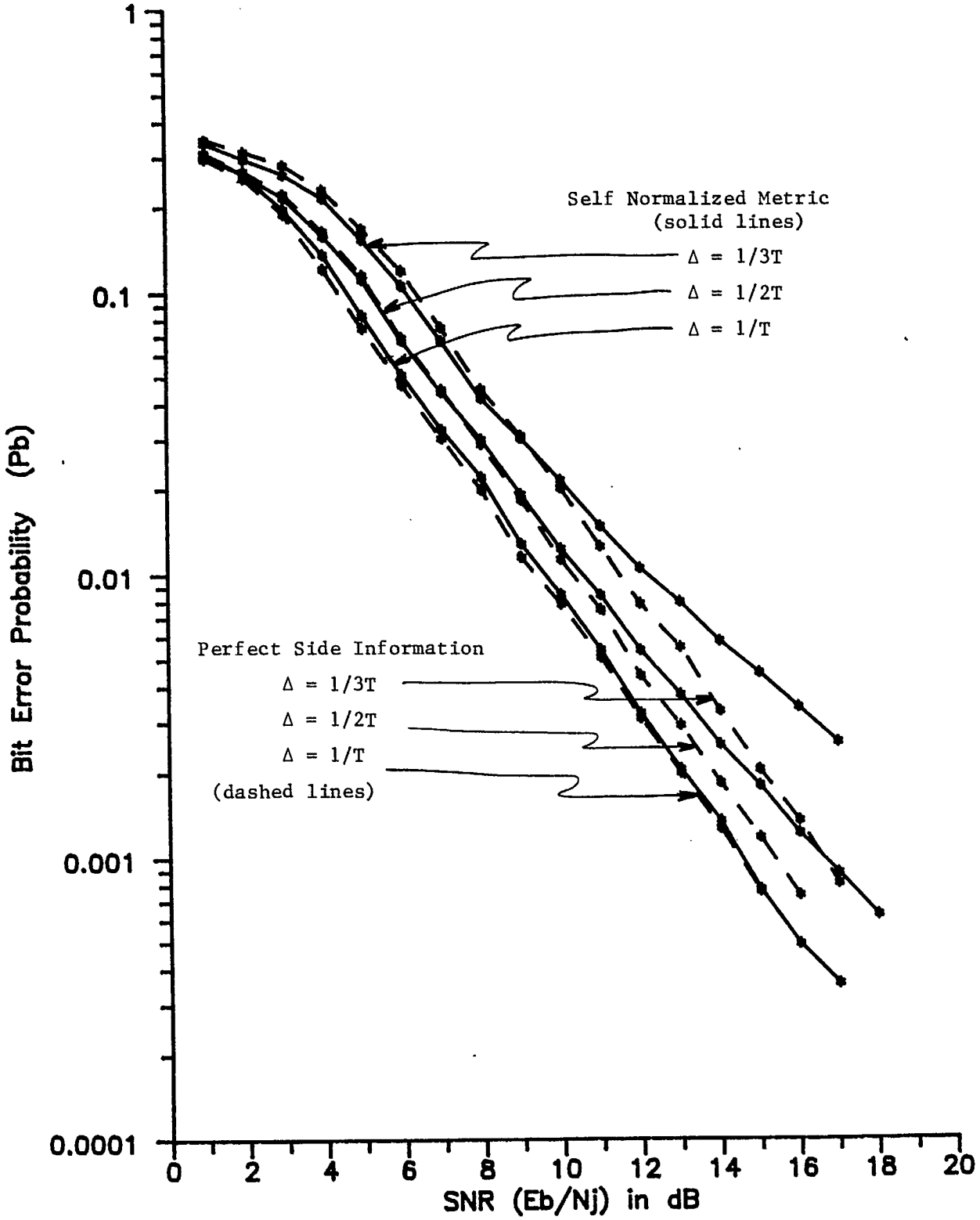

Figure 20 Comparison of 4-ary NC-FSK with 2 state trellis coding in partial band jamming using self normalized metric and using perfect side information.

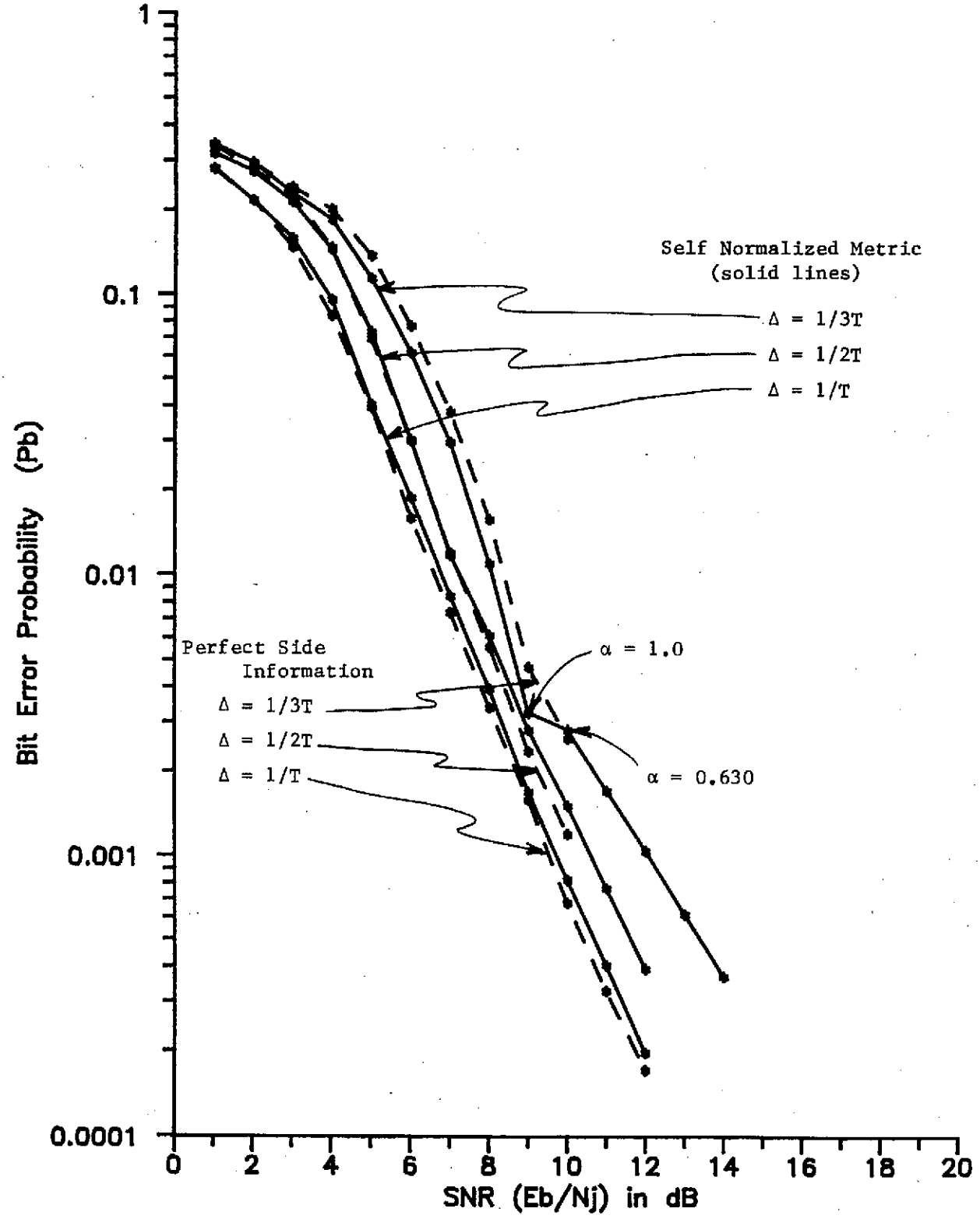

Figure 21 Comparison of 4-ary NC-FSK with 4 state trellis coding in partial band jamming using perfect side information and using the self normalized metric.

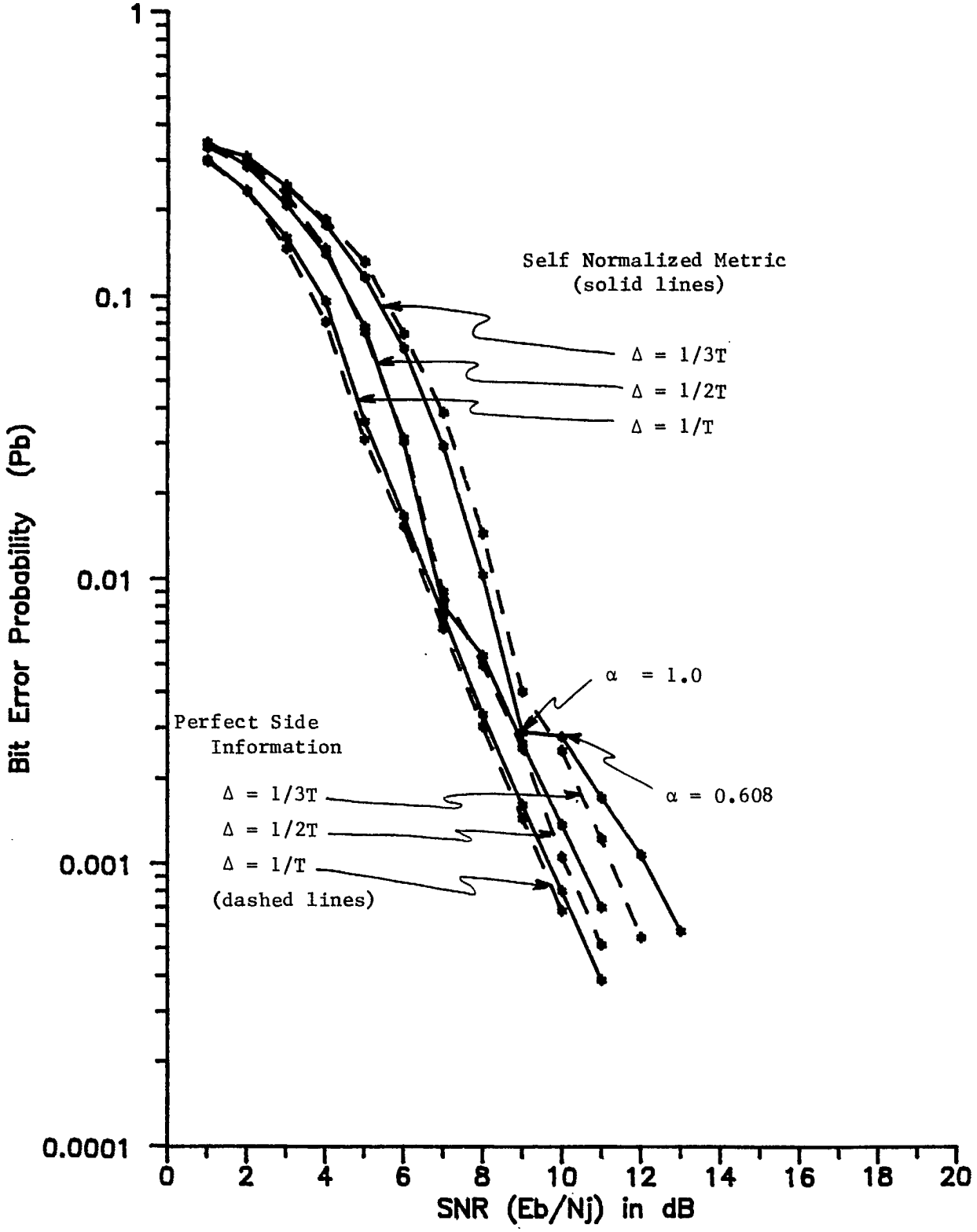

Figure 22 Comparison of 4-ary NC-FSK with 8 state trellis coding in partial band jamming using perfect side information and using the self normalized metric.

due to the fact that to set a tractable number of trials in the simulation the fraction of the band jammed (α) was taken from the bound on performance for perfect jammer side information. These regions coincide with the region where that bound changes quite rapidly from the situation where the full band is jammed to the case where only a fraction of the band is jammed.

V. CONCLUSIONS

In this report a frequency-hopped system with trellis-coded noncoherent frequency-shift-keying is presented. It is proposed that k bits per baud be encoded into a set of $m = 2^{k+1}$ NCFSK signals. Nonorthogonal tone spacing is considered to avoid bandwidth expansion. Following Ungerboeck's signal set partitioning method, the m-ary signals are partitioned into subsets. Soft decision decoding with a maximum metric decoder is employed. The metric considered in this report is the energy metric with perfect information as to the presence or absence of jamming in the band. As well for the jamming environment, a metric that divides the output of each of the energy detectors by the sum of their outputs is considered.

Performance analysis of the system under full-band and partial band noise jamming is presented. Theoretical results based on a new analysis of the Chernoff bound on pairwise error probability for energy detectors where the signals are correlated, is presented. The union Chernoff bound on bit error probability is derived utilizing the transfer function bounding technique. For an m-ary nonorthogonal signal set, there are (m-1) parameters D_k in the union Chernoff bound. The parameters D_k are formulated for partial band noise jamming and are used in the derivation of the transfer function bound on error performance, in place of the usual parameter D with squared distance exponent, which arises for coherent coded systems. For the codes under study, improvements in error performance and dramatic improvement in immunity to partial-band jamming is seen.

System performance is evaluated for 2-state, 4-state and 8-state trellis codes with tone spacings of 1/3T, 1/2T, 2/3T and 1/T Hz. Results are presented for a system both in additive white Gaussian noise and in a worst case partial band noise jamming environment. The use of a reduced

tone spacing instead of orthogonal tone spacing of 1/T Hz, brings little degradation in error performance, but a saving in bandwidth occupancy. A simulation of the system has been carried out and the theoretical results using bounds come within a fraction of a dB. of the simulations. Jammer side information derived in the receiver, yields substantial additional improvement in a jamming environment. The main part of this improvement can be seen with a practical implementation which passes normalized variables to the Viterbi decoder.

REFERENCES

1. P.H. Wittke and Y.M. Lam, A Study of Space Communications Spread-spectrum Systems - Part 2 Coding and Modulation Interim Progress Report for Dept. of Communications - Contract No. 36001-8-3528/01-ST, Queen's University, Dept. of Electrical Engineering Report No. 89-1, March, 1989.
2. M.K. Simon, J.K. Omura, R.A. Scholtz and B.K. Levitt, Spread Spectrum Communications, Vol. I, II and III, Computer Science Press, Inc., 1985.
3. R.E. Ziemer and R.L. Peterson, Digital Communications and Spread Spectrum Systems, Macmillan Publishing Company, Inc., 1985.
4. T.C. Huang and L. Yen, "Error Probability of a Noncoherent MFSK/FH Receiver in the Presence of Interference and Gaussian Noise," Proc. MILCOM'82, Boston, Mass., pp. 14.3.1-14.3.7, Oct. 17-20, 1982.
5. B.K. Levitt, "Use of Diversity to Improve FH/MFSK Performance in Worst Case Partial Band Noise and Multitone Jamming," Proc. MILCOM'82, Boston, Mass., pp. 28.2.1 - 28.2.5, Oct. 18-20, 1982.
6. Y.M. Lam, "High Data Rate Spread Spectrum Systems with Band-Efficient Modulations," Doctoral Dissertation, Department of Electrical Engineering, Queen's University, Kingston, Ontario, Canada, July 1988.
7. H.H. Ma and M.A. Poole, "Error-Correcting Codes Against the Worst-Case Partial-Band Jammer," IEEE Trans. on Commun., Vol. COM-32, No.2, pp.124-133, Feb. 1984.
8. W.E. Stark, "Coding for Frequency-Hopped Spread-Spectrum Communication with Partial-Band Interference - Part II : Coded Performance," IEEE Trans. on Commun., Vol. COM-33, No. 10, pp. 1045-1057, Oct. 1985.

9. K. Cheun and W.E. Stark, "Performance of Convolutional Codes with Diversity under Worst Case Partial-Band Noise Jamming," ICC'88 Proceedings, Philadelphia, PA., pp. 43.1.1-43.1.5, June 12-15, 1988.

10. L.E. Miller, J.S. Lee and A.P. Kadrichu, "Probability of Error Analyses of a BFSK Frequency-Hopping System with Diversity under Partial-Band Jamming Interference - Part III : Performance of a Square-Law Self-Normalizing Soft Decision Receiver," IEEE Trans. on Commun., Vol. COM-34, pp. 669-675, July 1986.

11. D.T. Torrieri, "Frequency Hopping with Multiple Frequency-Shift Keying and Hard Decisions," IEEE Trans. on Commun., Vol. COM-32, No. 5, pp.574-582, May 1984.

12. A.J. Viterbi, "A Robust Ratio-Threshold Technique to Mitigate Tone and Partial Band Jamming in Coded MFSK Systems," Proc. MILCOM'82, Boston, Mass., pp. 22.4.1 - 22.4.5, Oct. 18-20, 1982.

13. M.B. Pursley and W.E. Stark, "Performance of Reed-Solomon Coded Frequency Hop Spread-Spectrum Communications in Partial Band Interference," IEEE Trans. on Commun., Vol. COM-33, No.8, pp. 767-774, Aug. 1985.

14. S. Laufer and A. Reichman, "Analysis Of Frequency-Hopping Systems with Combined Convolutional and Diversity Encoding And Non-Ideal Interleaving in Worst Case Partial Band Jamming," ICC'88 Proceedings, Philadelphia, PA., pp. 43.2.1-43.2.5, June 12-15, 1988.

15. J.S. Lee, L.E. Miller and R.H. French, "Coded and Uncoded Performance of L-Hops/Symbol Frequency-Hopping Random MFSK Using a Nonlinear Diversity Combining Soft-Decision Schemes," ICC'87 Proceedings, Seatle, Washington, pp. 26.3.1-26.3.6, June 7-10, 1987.

16. D. Torrieri, "The Performance of Five Different Metrics Against Pulsed Jamming," IEEE Trans. on Commun., Vol. COM-34, No. 2, pp. 200-204, Feb. 1986.

17. P.J. Lee, "Performance of a Normalized Energy Metric without Jammer State Information for an FH/MFSK System in Worst Case Partial Band Jamming," IEEE Trans. on Commun., Vol. COM-33, No.8, pp. 869-877, Aug. 1985.

18. G. Ungerboeck, "Trellis-coded Modulation with Redundant Signal Sets - Part I : Introduction," IEEE Communication Magazine, Vol. 25, No. 2, pp.5-11, Feb. 1987.

19. J.L. Massey, "Coding and Modulation in Digital Communications," Proc. 1974 International Zurich Seminar on Digital Communications, Zurich, Switzerland, pp.E2(1)-(4), March 1974.

20. G. Ungerboeck, "Channel Coding with Multilevel/phase Signals," IEEE Trans. on Information Theory, Vol. IT-28, pp.55-67, Jan. 1982.

21. G. Ungerboeck, "Trellis-coded Modulation with Redundant Signal Sets - Part II : State of The Art," IEEE Communication Magazine, Vol. 25, No. 2, pp.12-21, Feb. 1987.

22. A.R. Calderbank and J.E. Mazo, "A New Description of Trellis Codes," IEEE Trans. on Information Theory, Vol. IT-30, pp. 784-791, Nov. 1984.

23. M.K. Simon and D. Divsalar, "A New Description of Combined Trellis Coding With Asymmetric Modulations," JPL Pulbication 85-45, July 15, 1985.

24. P.H. Wittke, P.J. McLane, S.J. Simmons, M.G. Wearring, Y.M. Lam and W. Hopkins, "The Study of Space Communications Spread Spectrum Systems (Phase IV)," Dept. of Elect. Eng., Queen's University, Research Report No.87-1, June 1987.

25. A.J. Viterbi and J.K. Omura, Principles of Digital Communication and Coding, New York : McGraw-Hill, 1979.

26. E. Biglieri, "High-Level Modulation and Coding for Nonlinear Satellite Channels," IEEE Trans. on Commun., Vol. COM-32, No.5, pp. 616-626, May 1984.

27. E. Zehavi and J.K. Wolf, "On the Performance Evaluation of Trellis Codes," IEEE Trans. on Information Theory, Vol. IT-33, No. 2, pp. 196 - 201, March 1987.

28. J.G. Proakis, Digital Communications, New York, McGraw-Hill, 1983.

29. M. Schwartz, W.R. Bennett and S. Stein, Communication Systems and Techiques, McGraw-Hill, 1966.

30. B.D. Trumpis, "On the Optimum Detection of Fast Frequency Hopped MFSK Signals in Worst Case Jamming," TRW Internal Memorandum, June 1981.

31. Q. Wang, T.A. Gulliver, V.K. Bhargava and D.W. Little, "Coding for Frequency Hopped Spread Spectrum Satellite Communications," Technical Report ECE-88-2, Dept. of Electrical and Computer Engineering, University of Victoria, April 1988.

APPENDIX A

CHERNOFF BOUND FOR NONCOHERENT M-ARY FSK

A.1 Nonorthogonal Signalling

To estimate the error performance for trellis coded M-ary noncoherent FSK, the Chernoff bound will be evaluated. In particular, we must evaluate (15)

$$D'(\lambda,\rho,q) = E\left\{e^{\lambda c(q)[e_j - e_i]}\Big| i,\ Q=q\right\}\ j \neq i, \tag{A.1}$$

where e_i and e_j are the outputs of the i^{th} and j^{th} energy detectors. The expectation can be evaluated fairly directly in the case where the tones are orthogonally spaced since the inphase and quadrature components of the energy detector outputs e_i and e_j are statistically independent [28]. However in the general case of nonorthogonal frequencies, of interest here, considerably more effort is required. Equation (A.1) appears similar in form to a moment generating or characteristic function of a Hermitian quadratic form of complex Gaussian random variables. Hence the technique used will be essentially that of finding such a characteristic function [29, p.590].

Suppose the i^{th} signal is sent

$$s_i(t) = A\cos(\omega_i t + \theta_i) \tag{A.2}$$

and the received signal is

$$r(t) = s_i(t) + n(t) \tag{A.3}$$

where n(t) is white Gaussian noise with mean zero and power spectral density of $N_o/2$ watts/Hz. The complex random variable Z_k associated with the k^{th} energy detector, as shown in Fig. A.1, is

$$Z_k = X_k + j\ Y_k \tag{A.4}$$

It will be convenient for analysis purposes to deal with normalized random variables

$$\zeta_k = 2\ Z_k/[N_o T]^{1/2}, \tag{A.5}$$

and these normallized variables may be used without altering decisions or the receiver performance. Then, given that signal $s_i(t)$ was sent, the random variables ζ_k have a mean

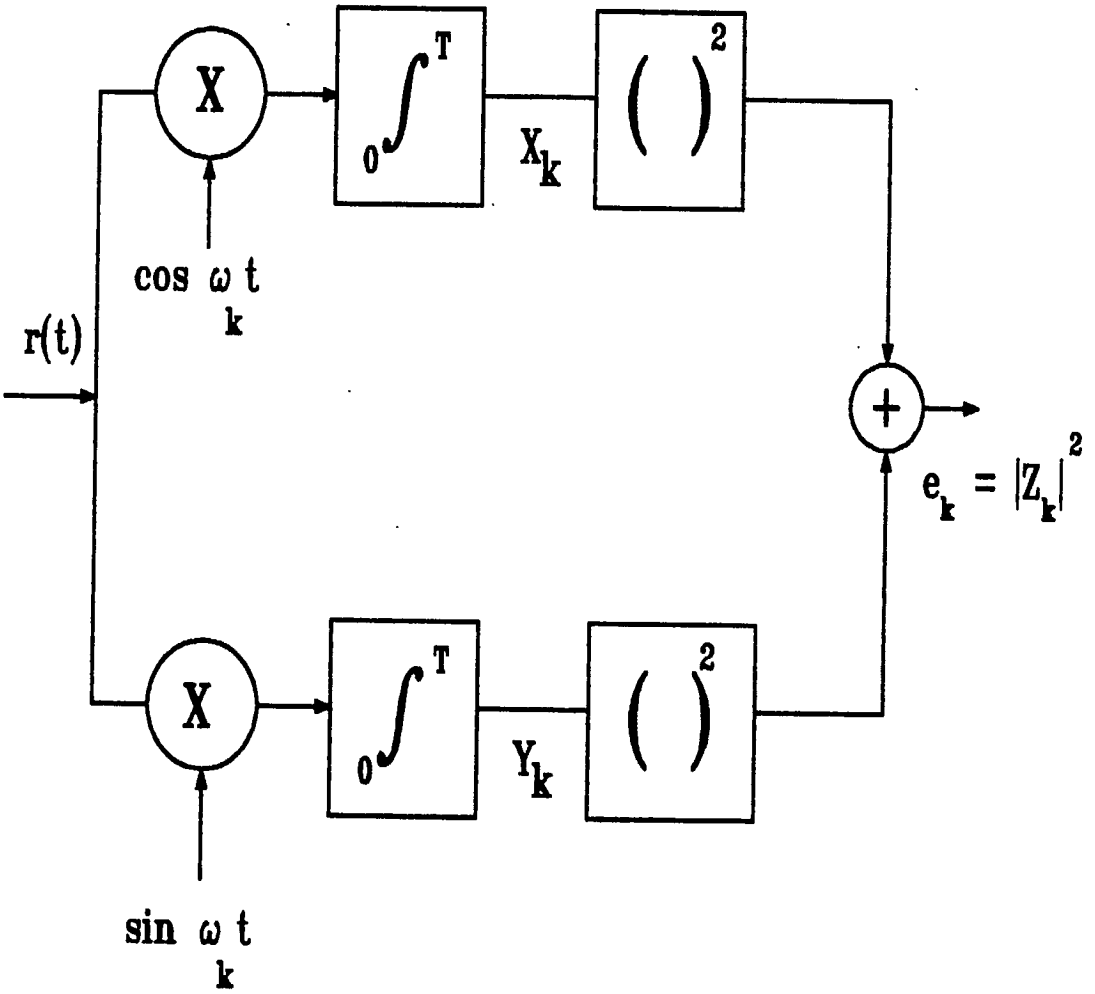

Fig. A.1 The k^{th} Energy Detector.

$$\mu_{\zeta_k} = E\{\zeta_k\} = [2\ E/N_o]^{1/2}\ \rho^* \tag{A.6}$$

where E the energy in the signal is $A^2T/2$, N_o is the single sided spectral density of the white noise in watts/Hz, and

$$\rho = \sin(\omega_k - \omega_i)T/(\omega_k - \omega_i)T + j\ [1 - \cos(\omega_k - \omega_i)T]/(\omega_k - \omega_i)T \tag{A.7}$$

In the calculation of the Chernoff bound, we will be dealing with the distribution of a Hermitian quadratic form of the random variables ζ_k and ζ_i, given $s_i(t)$ was sent. For notational simplicity, we will consider the vector

$$\underline{Z}^T = [\zeta_1,\ \zeta_2] \tag{A.8}$$

where T denotes the transpose. Then $\underline{Z}$ has a covariance matrix

$$\underline{R} = 1/2\ E\{[\underline{Z} - E\{\underline{Z}\}]^*\ [\underline{Z} - E\{\underline{Z}\}]^T\} \tag{A.9}$$

$$= \begin{bmatrix} 1 & \rho \\ \rho^* & 1 \end{bmatrix}$$

The Matrix $\underline{R}$ has eigenvalues $1 \pm |\rho|$. Thus a unitary transformation $\underline{U}$ can be formed, whose columns consist of the orthonormal eigenvectors of $\underline{R}$

$$\underline{U} = (1/\sqrt{2}) \begin{bmatrix} 1 & 1 \\ |\rho|/\rho & -|\rho|/\rho \end{bmatrix} \tag{A.10}$$

$$\underline{U}^{T*}\underline{U} = \underline{I} \tag{A.11}$$

where $\underline{I}$ is the identity matrix. The transformation $\underline{U}$ diagonalizes the covariance matrix $\underline{R}$

$$\underline{U}^{T*}\underline{R}\underline{U} = \underline{\Lambda} \tag{A.12}$$

$$\underline{R} = \underline{U}\underline{\Lambda}\underline{U}^{T*} \tag{A.13}$$

$$\underline{\Lambda} = \begin{bmatrix} 1 + |\rho| & 0 \\ 0 & 1 - |\rho| \end{bmatrix} \tag{A.14}$$

The problem of evaluating (A.1) can be viewed as that of evaluating the characteristic function of a Hermitian form

$$f = \underline{Z}^{T*}\underline{F}\ \underline{Z} \tag{A.15}$$

where in particular

$$\underline{F} = \begin{bmatrix} 1 & 0 \\ 0 & -1 \end{bmatrix} \tag{A.16}$$

The problem is solved by finding a transformation that simultaneously diagonalized both $\underline{R}$ and $\underline{F}$. Suppose we factor $\underline{\Lambda}$ in the form

$$\underline{\Lambda} = \underline{\Psi}^* \underline{\Psi}^T \tag{A.17}$$

where $\underline{\Psi}$ is the diagonal matrix with diagonal terms the square root of the corresponding diagonal terms of $\underline{\Lambda}$

$$\underline{\Psi} = \begin{bmatrix} (1 + |\rho|)^{1/2} & 0 \\ 0 & (1 + |\rho|)^{1/2} \end{bmatrix} \tag{A.18}$$

It can be verified directly that the transformation

$$\underline{W} = \underline{\Psi}^{-1} \underline{U}^T \underline{Z} \tag{A.19}$$

yields a Gaussian random vector $\underline{W}$ whose covariance matrix is the identity matrix. The inverse of this transformation is

$$\underline{Z} = \underline{U}^* \underline{\Psi} \underline{W} \tag{A.20}$$

and so the quadratic form (A.15) can be expressed as the Hermitian quadratic

form $$f = \underline{W}^{T*} \underline{T} \underline{W} \tag{A.21}$$

in the independent complex Gaussian variables $\underline{W}$,

where $$\underline{T} = \underline{\Psi}^{T*} \underline{U}^T \underline{F} \underline{U}^* \underline{\Psi} \tag{A.22}$$

As before, the quadratic form (A.21) can be expressed in terms of a diagonal matrix $\underline{\Phi}$ of the eigenvalues of $\underline{T}$

$$\underline{T} = \underline{S} \underline{\Phi} \underline{S} \tag{A.23}$$

where again $\underline{S}$ is a matrix whose columns are the normalized eigenvectors of $\underline{T}$. Thus with the transformation

$$\underline{\eta} = \underline{S}^{T*} \underline{W} \tag{A.24}$$

or $$\underline{W} = \underline{S} \underline{\eta} \tag{A.25}$$

the quadratic form (A.21) is diagonal

$$f = \underline{\eta}^{T*} \underline{\Phi} \underline{\eta} = \sum_{i=1}^{2} \Phi_i |\eta_i|^2 \tag{A.26}$$

and the covariance matrix of $\underline{\eta}$ is the identity matrix. Finally,

$$\underline{\eta} = \underline{S}^{T*} \underline{\Psi}^{-1} \underline{U}^T \underline{Z} \tag{A.27}$$

Let $$\eta_i = \alpha_i + j\,\beta_i, \qquad i = 1,2 \tag{A.28}$$

Then $$f = \sum_{i=1}^{2} \Phi_i (\alpha_i^2 + \beta_i^2) \tag{A.29}$$

and the probability density function of the α_i's and β_i's is

$$p(\alpha_1,\alpha_2,\beta_1,\beta_2) = (2\pi)^{-2} \prod_{i=1}^{2} \exp(-\{[\alpha_i - E\{\alpha_i\}]^2 + [\beta_i - E\{\beta_i\}]^2/2) \tag{A.30}$$

We require $E\{\exp(\lambda c(q)f)$ which can be evaluated from (A.29) and (A.30) to give [29, p.593]

$$E\{\exp(\lambda c(q)f)\} = \frac{\exp(\lambda c(q) \sum_{i=1}^{2} |E\{\eta_i\}|^2 \phi_i/[1 - 2\lambda c(q)]}{\prod_{i=1}^{2} [1 - 2\lambda c(q)\ \phi_i]} \tag{A.31}$$

Further manipulation of the matrices [29,p.594] yields equivalent expressions such as

$$E\{\exp(\lambda c(q)f)\} = \frac{\exp\ (\lambda c(q)\ E\{\underline{Z}^{T*}\}\ [\underline{F}^{-1} - 2\lambda c(q)\underline{R}^{*}]^{-1}E\{\underline{Z}\})}{\underline{I} - 2\lambda c(q)\ \underline{R}^{*}\underline{F})} \tag{A.32}$$

The particular form evaluated in the calculations was (A.31). First the eigenvalues of $\underline{T}$ were found

$$\phi_{1,2} = \pm\ (1 - |\rho|^2)^{1/2} \tag{A.33}$$

The terms $E\{\eta_i\}$ can be found from the relation

$$E\{\eta\} = \underline{S}^{T*}\ \underline{\psi}^{-1}\underline{U}^{T}E\{\underline{Z}\} \tag{A.34}$$

and after making use of the fact $\phi_1 = -\phi_2$, we end with the final expression

$$E\{\exp(\lambda c(q)f)\} = \frac{\exp(\ \frac{\lambda c(q)\ E}{4\quad N_o}\ [\frac{\phi_1\ |L_1|^2}{(1 - \lambda c(q)\phi_1)} - \frac{\phi_1|L_2|^2}{(1 + \lambda c(q)\phi_1)}])}{1 - \lambda^2\ c^2(q)\ \phi_1^2} \tag{A.35}$$

where $L_1 = \rho^{*}(a + b) + (|\rho|/\rho)\ (a - b)$

and $L_2 = \rho^{*}(a - b) + (|\rho|/\rho)\ (a + b)$

with $a = (1 + |\rho|)^{-1/2}$, and $b = (1 - |\rho|)^{-1/2}$ (A.36)

A.2 Orthogonal Signalling

In the case where the spacing between the NCFSK tones yields orthogonal signalling, the above derivation and results for the Chernoff bound simplify dramatically. Then

$$\underline{R} = \underline{I} = \underline{U} = \underline{\Lambda} \tag{A.36}$$

The eigenvalues of $\underline{T}$ are

$$\phi_1 = 1, \text{ and } \phi_2 = -1 \tag{A.37}$$

$$E\{\eta_1\} = 0, \text{ and } E\{\eta_2\} = (2\ E/N_o)^{1/2} \tag{A.37}$$

and we have the final result

$$E\{\lambda c(q) f\} = \frac{\exp\left(-\lambda c(q)\ (E/N_o)\ (1 + \lambda c(q))^{-1}\right)}{(1 - \lambda^2\ c^2(q))} \tag{A.38}$$